UNCLASSIFIED

AD NUMBER

AD054379

NEW LIMITATION CHANGE

TO

Approved for public release, distribution unlimited

FROM

Distribution authorized to U.S. Gov't. agencies and their contractors; Specific Authority; Dec 1953. Other requests shall be referred to WADC, Wright-Patterson, AFB OH.

AUTHORITY

AFAL ltr 17 Aug 1979

THIS PAGE IS UNCLASSIFIED

AN EXPERIMENTAL INVESTIGATION OF THE
USE OF HOT GAS EJECTORS FOR
BOUNDARY LAYER CONTROL

RICHARD V. DE LEO

RICHARD D. WOOD

UNIVERSITY OF MINNESOTA

DECEMBER 1953

WRIGHT AIR DEVELOPMENT CENTER

NOTICE

When Government drawings, specifications, or other data are used for any purpose other than in connection with a definitely related Government procurement operation, the United States Government thereby incurs no responsibility nor any obligation whatsoever; and the fact that the Government may have formulated, furnished, or in any way supplied the said drawings, specifications, or other data, is not to be regarded by implication or otherwise as in any manner licensing the holder or any other person or corporation, or conveying any rights or permission to manufacture, use, or sell any patented invention that may in any way be related thereto.

AN EXPERIMENTAL INVESTIGATION OF THE
USE OF HOT GAS EJECTORS FOR
BOUNDARY LAYER CONTROL

RICHARD V. DE LEO

RICHARD D. WOOD

UNIVERSITY OF MINNESOTA

DECEMBER 1953

AIRCRAFT LABORATORY
CONTRACT No. AF 33(038)-5131
TASK No. 13620

WRIGHT AIR DEVELOPMENT CENTER
AIR RESEARCH AND DEVELOPMENT COMMAND
UNITED STATES AIR FORCE
WRIGHT-PATTERSON AIR FORCE BASE, OHIO

FOREWORD

ABSTRACT

The primary purpose of Phase II of the ejector study has been to provide experimental data for engineering design purposes. The geometric and state parameters of the ejector were investigated over a wide range, both with and without diffuser. Variation in the ejector performance was determined for a change in primary temperature, and the effect of the use of a supersonic primary nozzle was also investigated. Comparisons of theoretical and experimental pumping performance without diffuser are presented.

PUBLICATION REVIEW

This report has been reviewed and is approved.

FOR THE COMMANDER:

D. D. McKee
Colonel, USAF
Chief, Aircraft Laboratory
Directorate of Laboratories

TABLE OF CONTENTS

LIST OF FIGURES

Effect of Primary Temperature Variation on Ejector Performance
(with diffuser)

Ejector Performance with a Supersonic Primary Nozzle (without diffuser)

L I S T   O F   T A B L E S

NOMENCLATURE

a   Local speed of sound.

a_o Stagnation speed of sound.

a_* Speed of sound where $M^* = 1.0$.

A_1 Exit cross-sectional area of primary nozzle.

A_3 Cross-sectional area of mixing tube section.

A_D Exit cross-sectional area of diffuser.

A^* Fictitious cross-sectional area of upstream throat where $M^* = 1.0$ for convergent nozzle $A_1^* = A_1$.

A_3/A_1 Area ratio of mixing tube to primary nozzle.

A_D/A_3 Area ratio of diffuser to mixing section.

D_1 Exit diameter of primary nozzle.

D_3 Diameter of mixing tube.

D_1^* Throat diameter of primary nozzle where $M_1^* = 1.0$.

F_e Total thrust of the ejector system in pounds.

F_J Total thrust of primary jet.

F_J' Thrust of primary jet produced by momentum.

ℓ Primary nozzle location in terms of mixing section diameters up or downstream of entrance to mixing section.

L   Mixing section length in terms of mixing section diameters.

L_x/D_1 Distance downstream of throat of primary nozzle in terms of throat diameters.

L_x/D_3 Distance downstream of entrance to mixing section length in terms of mixing section diameters.

m_1 Primary or jet mass flow in slugs per second.

m_2 Secondary mass flow in slugs per second.

m_3 Combined primary-secondary or ejector mass flow in slugs per second.

M^* Dimensionless velocity coefficient referred to the critical or throat speed of sound, a_*.

M_1^* Primary nozzle exit velocity coefficient.

M_2^* Secondary entrance velocity coefficient.

M_3^* Mixed flow exit velocity coefficient.

p_1 Static primary pressure.

p_2 Static secondary pressure.

p_3 Static pressure at exit of mixing tube.

p_x Static pressure along the mixing section length.

P_a Local atmosphere pressure.

P_1 Total primary pressure.

P_2 Total secondary pressure.

P_3 Total pressure at exit of mixing tube.

p_x/P_a Ratio of static pressure along mixing tube to atmospheric pressure.

P_1/P_a Ratio of total primary pressure to atmosphere pressure.

P_2/P_a Ratio of secondary total pressure to atmosphere pressure.

R Gas constant 1715 $ft^2 \ sec^2/R^o$.

t Static temperature.

T_a Ambient air temperature.

T_1 Total temperature of primary mass flow.

T_2 Total temperature of secondary mass flow (approximately equal to T_a).

T_3 Total temperature of mixed flow.

T_1/T_2 Ratio of primary to secondary temperatures T_1/T_a.

T_3/T_1 Ratio of mixed to primary temperatures.

V_1 Velocity of the primary jet mass flow.

V_2 Velocity of secondary mass flow, at entrance to mixing tube section.

V_3 Velocity of combined primary and secondary flow at the exit of the mixing tube.

W_1 Weight flow of primary stream in pounds per second.

W_2 Weight flow of secondary stream in pounds per second.

W_2/W_1 Weight or mass flow ratio of secondary to primary flows.

g 32.2 ft/sec^2.

γ Ratio of specific heats, c_p/c_v, (1.4 for air).

ρ Density of air in the free stream, slugs per cubic foot.

ρ_o Stagnation density of air, slugs per cubic foot.

ρ_* Density where $M^* = 1.0$.

S U M M A R Y

The primary purpose of Part II of the Hot Gas Ejector Investigation has been to obtain sufficient experimental data to allow the solution of practical design problems. The following general conclusions may be drawn from the data presented in Section III of this report:

A. **Ejector Pumping Performance**

1. For ejectors with and without diffuser a definite optimum ejector geometry, A_3/A_1, exists for any given set of primary and secondary state conditions to obtain a maximum mass flow ratio (secondary to primary). Conversely, for a given A_3/A_1 there exits an optimum primary pressure ratio in order to obtain maximum ejector performance.

2. For ejectors with and without diffuser the variation of ejector mass flow with secondary pumping ratio for a given ejector geometry is essentially linear for operation at primary pressures equal to or less than the optimum. At values in excess of the optimum the variation is slightly non-linear with increasing slope at higher secondary pumping ratios.

3. The addition of a diffuser at the mixing tube exit will improve ejector performance at values of primary pressure ratios below the optimum. At primary pressure in excess of the optimum, the performance of ejectors with and without diffuser tend to converge.

4. For a given ejector geometry with constant secondary and primary stagnation pressures the secondary weight flow is nearly proportional to the primary momentum. Thus, as the primary temperature is increased (at constant momentum) the weight flow ratio, W_2/W_1, increases approximately as $(T_1/T_2)^{1/2}$. In general, this approximation will over-estimate the effect of temperature.

5. On the basis of the one ejector geometry investigated, the use of a supersonic primary nozzle gave performance which was equal to or less than the performance of a sonic nozzle. However, for these experiments the supersonic nozzle was not designed to give a uniform parallel exit jet.

6. Ejector pumping performance may reasonably be predicted at large area ratios $A_3/A_1 > 4.0$, by the analytical method presented.

B. **Ejector Thrust Performance** (configurations without diffuser)

1. Ejector thrust is approximately linearly dependent on the mass flow ratio or secondary pressure ratio for a given geometry and primary operating conditions.

2. The slope of the thrust-secondary pressure ratio curve is dependent upon ejector geometry, A_3/A_1, and essentially independent of primary operating conditions, temperature and pressure.

3. On the basis of the one ejector geometry investigated, the use of a supersonic primary nozzle operating at design Mach number, gave a substantial increase in ejector thrust at a constant secondary pressure ratio as compared to the sonic nozzle. For operating conditions with incomplete supersonic expansion to the nozzle exit, the thrust was equal to or less than the sonic value.

The ejector pumping and thrust performance data obtained should be sufficient to solve most boundary layer design problems utilizing a turbo-jet engine for primary ejector power. The principle unknown factor in such applications is the importance of scale effect. Apparently little experimental work has been done on the subject. It is recommended that an experimental study of scale effect be initiated including operation with a full-scale turbo-jet engine.

I. INTRODUCTION

During the recent years the use of boundary layer control on aerodynamic surfaces for the reduction of air flow separation has become increasingly important. The control of the boundary layer may be accomplished by surface air removal in which case the growth of boundary layer is regulated. The addition of energy to the boundary layer by means of a blowing slot or jet is also a practical control device. In either case the resulting aerodynamic increase in lift or a decrease in drag is of prime importance. Of course, the ultimate economy of any boundary layer control system depends on the gain in aerodynamic performance as opposed to the added weight, power and complexity of the control system. A possible source of power for control is the inductive capacity of an ejector configuration using either exhaust gas or compressor air from a turbo-jet engine.

Results from Part I of this investigation, reference 2, indicated that adequate capacity for boundary layer control could be obtained with certain ejector configurations. For constant primary operating conditions, ejector performance was relatively insensitive to the geometric parameters of primary nozzle location and mixing section length. The results show that any ejector pumping action is usually accompanied by a decrease in thrust. It was also evident that an optimum geometry exists for each combination of flow conditions.

The present investigation is an extension of the work previously done. The geometric and state parameters of the ejector were investigated over a wide range, both with and without diffuser. Variation in ejector performance was determined for a change in primary temperature. The use of a supersonic primary nozzle was also investigated. Comparisons of theoretical and experimental ejector pumping and thrust performance without diffuser are presented.

II. DESCRIPTION OF APPARATUS

Photographs of the apparatus and its components, and a schematic drawing of the test installation are presented as Figures 1 through 3.

In order to obtain a high temperature primary jet a TG-180 combustion chamber was used to which was attached a convergent exit nozzle of circular cross section. Equipped with the conventional spray fuel nozzle and spark ignition, the chamber was mounted upon a free-moving thrust table (Figure 1).

A large plenum chamber made up of a section of 20-inch diameter steel pipe was mounted around the exhaust nozzle and combustion chamber, and was sealed around the burner on one end. Besides acting as a plenum for the induced secondary air, it served as a mount for the entrance cone and mixing tube of the ejector. The entrance cone of the ejector was sealed to the plenum chamber by means of a rubber "O" ring with the cone being adjustable horizontally to allow for variations in primary nozzle location. The ejector entrance cone and mixing tube were also fastened to the thrust table. The table was restrained in the thrust direction by a small cantilever beam mounted with a pair of strain gages. Strain in the beam caused a change in electrical resistance of the gages with a consequent unbalance in a wheatstone bridge circuit. The unbalance was indicated by deflection of a sensitive galvanometer. This deflection was statically calibrated in terms of pounds of thrust.

The diffuser sections of the ejector were of the conical type with a 7-degree wall divergence. They were constructed from 10-gauge sheet steel and were fastened to the mixing tube by means of flanges.

Primary air was obtained from several air compressors capable of producing 110 pounds per square inch gage pressure, while delivering a mass of air of approximately 4.5 pounds per second per compressor. Induced air was taken from the atmosphere through two secondary inlet pipes. The mass flows of primary and secondary air were measured by orifice plates and controlled by separate valves.

Spark ignition was obtained from a 12,000 volt transformer with kerosene being used as fuel. A temperature cut-off and Mercury pressure switch were used in the fuel-line as safety devices.

Temperature measurements were made by means of thermocouples connected to a 24-channel Brown 0° to 2000° Fahrenheit potentiometer. Pressures were read by Bourdon gages, Merriam differential manometers and standard U-tubes.

III. EXPERIMENTAL RESULTS

The test results may logically be divided into five separate sections, each of which is discussed below. In each section, data was obtained for several ejector configurations over a range of state and flow conditions. Nomenclature, and the approximate location of the points of measurement are shown in Figure 4. In the majority of the tests, data was obtained for five conditions of secondary mass flow and stagnation pressure.

Thrust and mass flow measurements were made at primary pressure ratios ranging from $P_1/P_a = 1.25$ to 5.00 without the ejector system to check primary nozzle operation. The results were corrected to a standard condition of primary stagnation temperature, $T_1 = 1200^\circ F$, and a barometric pressure of $P_a = 29.92"$ Hg. Experimental results were compared with theoretical values calculated for the standard conditions in Figures 5 and 6. Good agreement between the actual and theoretical values was obtained. The mass flow was plotted in terms of (W_1/A_1) where $A_1 = 11.7$ square inches.

A. Ejector Without Diffuser

A series of tests were made without diffuser at the exit of the mixing tube. Since the previous investigation, (reference 2), indicated that a variation of primary nozzle location had little effect upon ejector performance this parameter was held constant with the exit of the primary jet in the same plane as the entrance to the mixing tube ($\ell = 0$). Based on the results of reference 2, the mixing tube length was also maintained at 7.5 diameters for this investigation.

1. Ejector Pumping Performance

Ejector pumping performance without diffuser was determined over a range of mixing tube to primary nozzle area ratios from A_3/A_1 = 1.21 to 6.00 at primary pressure ratios within the range of P_1/P_a = 1.25 to 5.72. The primary to secondary total temperature ratio was maintained constant at T_1/T_2 = 3.32 for most of the tests as this corresponds to jet engine exhaust temperature. Exceptions are noted specifically on the individual data plots. This particular temperature ratio was used because it gives a value of T_1 = 1200°F which represents the maximum turbine discharge temperature of current turbojet engines. Test results showing the effect of a change in primary pressure ratio on ejector performance are shown in the top graph of Figures 7 through 21. The variation in primary to secondary mass flow ratio (W_2/W_1) versus secondary pressure ratio has been plotted for lines of constant primary pressure ratio. In this series of tests on the mixing tube area was changed.

These test data indicate the following general trends:

a. The variation of mass flow ratio with secondary pressure ratio is essentially linear at low primary pressure ratios.

b. The slope of the mass flow ratio – secondary pressure ratio curves decrease with increasing primary pressure ratio for a given area ratio.

c. The slope of the mass flow ratio – secondary pressure ratio curves decrease with decreasing area ratio at a given primary pressure ratio.

d. For a given ejector configuration an optimum primary pressure ratio exists to give a maximum weight flow ratio at a given secondary pressure ratio.

e. At primary pressure ratios in excess of the optimum, the variation of mass flow ratio with secondary pressure ratio is non-linear.

It is evident from the data presented that the ejector performance (as indicated by the weight flow ratio at a given secondary pressure ratio) at first increases with increasing primary pressure ratio, reaches an optimum value and then decreases in all cases. In the case of $A_3/A_1 = 1.21$, $P_1/P_A = 2.00$ gives near optimum performance over the whole operating range of the ejector. In the case of the higher area ratio, i.e., $A_3/A_1 = 2.48$, the optimum pressure ratio shifts to lower values as the mass flow ratio is increased.

This optimum primary pressure ratio may be easily visualized from a cross plot of secondary pressure ratio versus primary pressure ratio for lines of constant mass flow ratio. This has been done for $A_3/A_1 = 1.72$, 2.48 and 4.30, and are shown in Figures 23 through 25. The dashed lines indicate operation with diffuser and will be discussed in Section B. The optimum value of the primary pressure ratio occurs where the secondary pressure ratio is a minimum. This minimum secondary pressure ratio increases as the mass flow ratio is increased and is reached at a lower value of primary pressure ratio.

An additional cross plot of the experimental performance data is presented as Figures 26 through 29. In these cases the primary jet operating parameters (temperature and pressure) are held constant and ejector mass flow ratio is plotted versus area ratio for lines of constant secondary pressure ratio. Data was obtained for area ratios $A_3/A_1 = 1.21$, 1.41, 1.72, 2.10, 2.48, 3.39, 4.30 and 6.00. By use of the curves it is possible to determine the maximum mass flow ratio for a given secondary pressure ratio and the area ratio at which it occurs for constant primary jet conditions. We may note, that as the primary pressure ratio is increased the maximum mass flow ratio increases and is produced at a higher area ratio for a constant secondary pressure ratio.

The existance of an optimum pressure ratio for a given geometry and weight flow ratio can probably be attributed to the following counter balancing effects:

a. With increasing primary pressure ratio the momentum per unit mass of primary flow is increasing. The effects of this increase in pressure is to decrease the secondary pressure ratio for a given mass flow ratio since more primary momentum per unit mass is available for pumping.

b. As the secondary pressure ratio decreases at constant mass flow ratio the secondary flow Mach number increases at the mixing tube entrance. At supercritical primary pressure ratios and above, the expansion of the primary jet leaving the sonic nozzle causes a further increase in the secondary flow Mach number and possibly even choking.

2. Ejector Thrust Performance

Ejector thrust was also determined over the pumping performance range by means of a simple strain gage balance system. The test results are shown in the lower graph of Figures 8 through 22. The ejector thrust in pounds has been plotted against secondary pressure ratio at lines of constant primary pressure ratio, P_1/P_A. Superimposed are lines of constant thrust ratio, F_e/F_j, which represent the ratio of measured ejector thrust to measured primary jet thrust.

It is evident from the test results that as the secondary pressure ratio is decreased, a linear decrease in thrust occurs. Since for a given ejector geometry the lines are approximately parallel, it appears that the absolute loss in thrust for a given secondary pressure ratio is independent of the primary pressure ratio. It may be noted that the slope of the thrust curve decreases as the area ratio A_3/A_1 is decreased.

B. Ejector With Diffuser

Ejector pumping performance with a diffuser at the exit of the mixing tube has been determined. The diffuser was of the simple conical type with an included angle of 7 degrees. In most cases the diffuser exit to entrance area ratio was held constant at $A_D/A_3 = 6.25$.

In an effort to determine only the effect of the addition of a diffuser, the mixing tube length was held constant at $L = 7.5 D_3$, (the same as for tests without a diffuser). The primary nozzle location remained at $(\ell) = 0$. The use of a diffuser, of course, eliminates the thrust of the system.

1. Ejector Pumping Performance

The pumping performance of an ejector with diffuser has been determined with $A_3/A_1 = 1.72$, 4.30, 8.60 and 12.00. Area ratios of $A_3/A_1 = 8.60$ and 12.00 were obtained by the use of a primary nozzle with one-half of the area previously used, that is, $D_1 = 2.73"$ instead of $D_1 = 3.86"$. The results of these tests are shown in Figures 30 through 34. For a constant primary temperature ratio of $T_1/T_2 = 3.32$, the primary pressure ratio was varied from $P_1/P_a = 1.25$ to 6.50.

The test data presented indicate the same general performance characteristics as noted and discussed in Section A-1. The existance of an optimum primary pressure ratio yielding maximum weight flow ratio at a given secondary pressure ratio is again evident. However, for $A_3/A_1 = 12.00$ the optimum pressure ratio has not been reached over the range investigated.

2. Comparison of Ejector Performance With and Without Diffuser

A comparison of ejector performance with and without diffuser is shown in Figures 23 through 25, where the secondary pressure ratio is plotted versus the primary pressure ratio for lines of constant mass flow ratio. The dashed lines indicate operation with diffuser and the solid lines an identical configuration without diffuser. It is apparent that with diffuser the optimum primary pressure ratio for a given mass flow ratio occurs at a lower value for all experimental data plotted. At primary pressure ratios near and below the optimum a substantial reduction in secondary pressure ratio may be obtained by use of a diffuser. At primary pressure ratios in excess of the optimum the performance of the two ejectors converge and become essentially equal in the case of area ratio

1.72 and 2.48, Figures 23 and 24. In the case of area ratio 4.30, Figure 25, the performance curve of the ejector with diffuser will apparently intercede the non-diffuser configuration at primary pressure ratios in excess of the optimum. It should be noted, however, that test data for the diffuser case was obtained only at P_1/P_a = 1.5, 2.0, 3.0 and 4.0, so these curves are not well defined.

In conclusion it may be stated that if thrust is unimportant, the ejector with diffuser shows superior performance at primary operating pressures below or near the optimum.

Ejector with diffuser performance data has been cross plotted in Figures 35 through 38, relating ejector mass flow ratio, area ratio and secondary pressure ratio at P_1/P_a = 1.5, 2.0 and 3.0 at T_1/T_2 = 3.32. Test data was available only at A_3/A_1 = 1.72, 2.48, 4.30, 6.00 and 12.00 so that the curves are not well defined, but may be sufficient for ordinary engineering purposes. The curves are similar to those obtained without diffuser.

C. The Effect of Primary Air Temperature on Ejector Performance

In order to evaluate the effect of primary air temperature on ejector performance over a range of geometric and state conditions tests were con-ducted at several ejector area ratios, A_3/A_1, and primary pressure ratios, P_1/P_a. Experiments were made on configurations with and without diffuser over a temperature range of T_1/T_2 from 1.0 to approximately 3.37. A tab-ulation of test runs including area ratios, primary pressure ratios and primary to secondary temperature ratios is given as Table I. A few representative results are plotted as Figures 39 through 46 for configurations without diffuser and Figures 47 through 50 for configurations with diffuser.

1. Ejector Pumping Performance

With reference to the above Figures it is readily seen that the effect of increase in primary temperature is to increase the mass flow ratio W_2/W_1 at any secondary pressure ratio, P_2/P_a, except at P_2/P_a corresponding to

$W_2/W_1 = 0$. In other words, the effect of heat addition to the primary stream is to increase the slope of the weight flow ratio - secondary pressure ratio curves. The intercept at $W_2/W_1 = 0$ remains unchanged. A tabulation of these slopes is included in Table I for all configurations investigated. In cases where the slope was not a constant as in Figure 41, comparisons were made at high flow ratios where the slope for a given temperature ratio is nearly constant. The slopes of performance lines at elevated primary temperatures are also expressed as multiples of the performance slope with unheated primary, $T_1/T_2 = 1.0$.

It is apparent from the results summarized in Table I, that the experimental program has served to spot the effect of heat addition to the primary flow under a variety of geometric and state conditions. Sufficient data is not available to indicate any exact or well defined trends. It appears from the results of Table I, that the secondary mass flow (not the mass flow ratio as indicated by the preliminary tests of reference 2) is proportional to the primary momentum. Thus, at constant primary total pressure ratios, P_1/P_a, the momentum remains unchanged with increasing temperature ratio (Appendix A) however, the primary mass flow is decreasing as $1/(T_1/T_2)^{1/2}$. If the secondary mass flow is proportional to the primary momentum, the mass flow ratio would then increase as $(T_1/T_2)^{1/2}$. With reference to Table I, the square root variation is in reasonable agreement with the results tabulated. However, in almost all cases the square root variation over estimates the effect of a temperature ratio variation.

2. Ejector Thrust Performance

The effect of a variation in primary temperature on ejector thrust (without diffuser) appears to be somewhat variable, Figures 40 through 46. In the case of $A_3/A_1 = 1.72$ at $P_1/P_a = 1.50$, Figure 41, the effect of a temperature ratio variation is small. However, for the data presented, the effect of an increase in temperature ratio is to cause a decrease in ejector thrust. This phenomenon (encountered previously, reference 2) can probably be attributed to increased mixing tube losses at the higher mixing tube velocities with increasing temperature ratio. It may be noted that the thrust loss is relatively constant over the whole range of ejector operation.

TABLE I

SUMMARY OF EXPERIMENTAL RESULTS FOR THE EVALUATION OF THE EFFECTS OF PRIMARY - SECONDARY TEMPERATURE RATIO

A_3/A_1	P_1/P_A	T_1/T_2	M_a	T_1/T_2	M_b	M_b/M_a	T_1/T_2	M_c	M_c/M_a	T_1/T_2	M_d	M_d/M_a
WITHOUT DIFFUSER												
1.72	1.50	1.00	0.665	1.65	0.840	1.262	2.47	0.946	1.422	3.26	1.040	1.564
1.72	2.00	1.00	0.345	1.65	0.490	1.420	2.47	0.561	1.627	3.25	0.569	1.650
1.72	3.00	1.00	0.286	1.65	0.369	1.290	2.42	0.434	1.515	3.19	0.467	1.632
2.10	2.00	1.00	0.711	1.64	0.816	1.150	2.40	0.950	1.338	3.32	1.011	1.424
2.48	1.50	1.00	0.764	1.72	2.09	1.184	2.52	2.41	1.366	3.32	2.73	1.547
2.48	3.00	1.00	0.542	1.72	0.684	1.262	2.52	0.842	1.553	3.32	0.905	1.670
4.30	1.50	1.00	6.01	1.64	7.59	1.261	2.40	8.56	1.424	3.16	8.56	1.424
4.30	2.50	1.00	2.32	1.64	2.86	1.233	2.40	3.21	1.373	3.16	3.69	1.590
4.30	3.50	1.00	1.26	1.64	1.50	1.190	2.40	1.76	1.397	3.16	1.90	1.509
WITH DIFFUSER												
1.72	2.00	1.00	0.476	1.72	0.559	1.174	2.50	0.591	1.241	3.37	0.574	1.205
2.48	2.00	1.00	0.895	1.72	1.123	1.257	2.52	1.455	1.625	3.32	1.546	1.728
4.30	2.00	1.00	6.43	1.64	7.61	1.183	2.40	8.57	1.333	3.16	10.46	1.728
8.60	2.00	1.00	25.90	2.00	35.00	1.351				3.32	40.4	1.560
8.60	4.00	1.00	7.30	2.00	9.55	1.308				3.32	10.2	1.397

T A B L E I I

EFFECT OF PRIMARY TEMPERATURE ON EJECTOR THRUST - $p_2/P_a = 0.80$

A_3/A_1	P_1/P_a	$(F_e)_{T_1 = T_a}$	$(F_e)_{T_1 = 3.3 T_a}$	ΔF_e	$\Delta F_e/(F_e)_{T_1 = T_a}$
		lb	lb	lb	
1.72	1.50	127	127	0	0
1.72	3.00	490	470	20	0.041
2.10	2.00	232	228	4	0.017
2.48	1.50	150	132	18	0.120
2.48	3.00	440	420	20	0.045
4.30	2.50	260	280	20	0.077

An ejector thrust comparison for several ejector geometries is given in Table II at a constant secondary pumping ratio, $P_2/P_a = 0.80$. It is evident from the table that at the higher primary pressure ratios for $A_3/A_1 = 1.72$, 2.48 and 4.30, the absolute magnitudes of the thrust losses are equal. At the lower primary pressure ratios there appears to be an increase in ΔF_e with increasing area ratio, however, the loss at $A_3/A_1 = 2.48$, $P_1/P_a = 1.50$ (18 lb) appears excessive. From Figure 44 it can be noted that thrust data for $T_1/T_a = 3.32$ is considerably displaced from the other three, and therefore subject to question.

D. Ejector Performance with Supersonic Primary Nozzle

For a limited number of tests the effect of the use of a supersonic primary nozzle on ejector performance was determined. For these tests, the 3.86-inch exit diameter sonic nozzle described in Section II was replaced by a supersonic nozzle of 3.94-inch throat diameter. Since these tests were

of an exploratory nature, the nozzle was of simple construction and not
designed to give uniform parallel flow at the nozzle exit. Use of a
parallel flow nozzle appeared unnecessary since the nozzle would operate
correctly only at design static pressure at the entrance to the ejector
mixing tube. At values below design static pressure the flow would
expand to a higher supersonic value, and at values above design pressure
the flow would probably separate from the nozzle walls through oblique
shock patterns.

Tests were initiated with a $M = 2.5$ supersonic primary nozzle.
However, it was determined from the results that design Mach number at the
nozzle exit could not be obtained when installed in the ejector because of
insufficient compression ratio.

Further experiments were conducted with the same nozzle with reduced
exit area to give a Mach number of approximately $M = 2.0$. These tests were
conducted at three primary pressure ratios, $P_1/P_A = 2.0$, 3.0 and 4.0 at
$T_1/T_A = 3.32$ using the 8-inch mixing tube with $A_3/A_1^* \cong 4.30$. Tests were run
at three axial nozzle positions, $\ell = 0$, $-0.072 \, D_3$, and $-0.25 \, D_3$. The
position $\ell = -0.072 \, D_3$ was selected so that A_2/A_1^* was equal to the sonic
nozzle case, $A_2/A_1 = 3.30$. Experimental data are presented as Figures 51
through 55.

The results presented as Figure 51 show that in all cases the pumping
performance of the ejector with $M = 2.0$ primary nozzle is equal to or less
than the performance with sonic nozzle. The effect of nozzle position is
apparently slight since all test points fall on essentially the same curve.

At a low primary pressure ratio, $P_1/P_a = 2.0$, the performance with
supersonic nozzle is consistently lower than the sonic. The fact that the
flow did not expand to the nozzle exit as shown in Figure 53 may be the
reason for this decrease. At higher primary pressure, $P_1/P_a = 3.0$, the
performances are essentially equal below a weight flow ratio of 0.500 with
the sonic nozzle being considerably superior above this value. With
reference to Figure 54, it is seen that $W_2/W_1 = 0.481$, the flow does not
expand to the nozzle exit. This again may account for the difference.

At P_1/P_a = 4.0 the same trends as at P_1/P_a = 3.0 are apparent but with smaller differences existing beyond W_2/W_1 = 0.500. The nozzle Mach number distribution shows full expansion to the nozzle exit for all test conditions, Figure 55.

An experimental thrust comparison between the two nozzle configurations is presented as Figure 52. From the results it is obvious that at higher primary pressure ratios, P_1/P_a = 3.0 and 4.0 large thrust increases over the sonic nozzle may be realized. From an analytical standpoint these results are difficult to verify. If the assumptions given in Appendix A are fulfilled the ejector thrust may be calculated from Equation 6.07. Thus, at equal mass flow ratios for a given set of primary conditions one would expect equal thrusts. As a check on the thrust, measurements of the total and static pressure distributions at the mixing tube exit were made by means of movable probe. (Typical distributions are presented in Section III-E). From the point by point total and static pressure measurements, an average mixing tube exit dimensionless velocity, M_3^*, was determined. Values of thrust were computed using equation 6.07 of Appendix A. In the case of sonic nozzle good agreement between measured experimental thrust and those calculated by using probe data was obtained. In the case of the supersonic nozzle an increase in thrust over the sonic nozzle was indicated by the calculated thrust, but the direct measured values of thrust were still higher. Profile data indicated. higher values of total pressure and lower static pressures for the supersonic nozzle case. Thus, an assumption of Appendix A that the static pressure at the end of the mixing be equal to atmospheric, (P_a), was violated and the mixed flow was partially supersonic.

To more fully understand the effect of the supersonic primary nozzle on ejector thrust it appears that further tests should be iniated.

E. Comparison of Experimental Data and Theoretical Analysis

A one-dimensional, a steady flow, a compressible analysis of ejector performance without diffuser has been made. Wall friction, nozzle shock, and mixing losses were neglected. It has also been assumed that mixing was completed within the ejector system.

Exit Velocity

$$S(M_3{}^*) = \frac{P_1}{P_a} \theta(M_1{}^*)\left(1 + \frac{W_2}{W_1}\right)\sqrt{\frac{T_3}{T_1}}\,\frac{A_1}{A_3}$$

where

$$S(M_3{}^*) = \theta(M_3{}^*)\frac{P_3}{P_3} = f(M_3{}^*)$$

Secondary Velocity

$$\frac{W_2}{W_1}\sqrt{\frac{T_2}{T_1}}\left(M_2{}^* + \frac{1}{M_2{}^*}\right) + \left(M_1{}^* + \frac{1}{M_1{}^*}\right) = \left(1 + \frac{W_2}{W_1}\right)\sqrt{\frac{T_3}{T_1}}\left(M_3{}^* + \frac{1}{M_3{}^*}\right)$$

Secondary Pumping Pressure

$$\frac{P_2}{P_a} = \frac{\dfrac{W_2}{W_1}\sqrt{\dfrac{T_2}{T_1}}\dfrac{P_1}{P_a}\theta(M_1{}^*)\dfrac{A_1}{A_2}}{\theta(M_2{}^*)}$$

Ejector-Jet Thrust Ratio

$$\frac{F_e}{F_j} = \frac{\dfrac{F_e}{F_j}}{1 + \dfrac{\left(\dfrac{P_1}{P_1} - \dfrac{P_a}{P_1}\right)}{\left(\dfrac{2\gamma}{\gamma+1}\right)\left(\dfrac{2}{\gamma-1}\right)^{\frac{1}{\gamma-1}}\theta(M_1{}^*)M_1{}^*}}$$

Valid for $P_1/P_a > 1.89$ and $\gamma = 1.4$

The derivation of these equations is given in Appendix A. It is apparent from these equations that knowledge of the primary flow conditions and the selection of the mass flow ratio (W_2/W_1) enables us to determine the exit and secondary flow conditions.

Theoretical ejector performance was calculated by means of these equations and it is compared with experimental data in Figures 56 through 59. With reference to the above Figures the following general conclusions may be drawn:

1. An optimum primary pressure ratio is predicted by the calculated performance curves which are in reasonable agreement with the experimental values at higher area ratios.

2. Best agreement between calculated and experimental performance was obtained at high area ratios and at low primary pressure ratios. The effect of area ratio is predominant so that at $A_3/A_1 > 4.0$, reasonable agreement was obtained under all ejector operating conditions.

From the above conclusions it appears that good agreement between actual and calculated performance is obtained at low mixing section velocities. Increasing the mass flow ratio, decreasing the area ratio, or increasing the primary pressure ratio all have the effect of increasing the mixing tube velocities and associated losses. Shock losses following over-expansion of the primary jet leaving the sonic nozzle are also increased with increasing primary pressure ratio. One shortcoming of the analysis may be in the fact that over-expansion of the primary jet is considered part of the mixing process. However, the inclusion of this effect would considerably complicate the analysis, and has not been included to date.

Experimental ejector thrust performance is compared with the theoretical values in Figures 60 through 63. The comparison is made between actual and theoretical values of ejector thrust, F_e, versus the mass flow ratio for lines of constant primary pressure ratio. Experimental values are shown as solid lines and the theoretical with dashed lines. The same values of $A_3/A_1 = 1.72$, 2.48 and 6.00 are used as in Figures 56 through 59.

Analysis of the curves indicates reasonable agreement of the experimental and theoretical ejector thrust values at a mass flow ratio of $W_2/W_1 = 0$. As the mass flow ratio is increased a rather consistent disagreement of the two values occurs with the experimental indicating a higher value. The difference appears to increase as the mass flow ratio becomes larger. No consistent trend is apparent as to the differences between experimental and theoretical ejector thrust as effected by a change in primary pressure ratio.

An examination of the total pressure distribution across the mixing tube exit, shown for A_3/A_1 = 4.30 in Figures 64 through 66, shows a decided displacement from the theoretical linear profile. Since this is a direct indication of a non-linear velocity distribution at the exit of the mixing tube, the thrust must be calculated point by point. It may be shown that since the thrust varies as the square of the velocity, a point by point summation of the thrust will be larger than that obtained by using an average velocity. Therefore, the velocity profile must be considered when calculating the ejector thrust.

Conditions at the exit of the mixing tube were investigated by means of surveys across the exit with a total pressure and total temperature probe. The results of these tests are shown in Figures 64 through 69 where the chain line indicates the theoretical one-dimensional value. The displacement of the total pressure curves from the theoretical appears to be an indication that mixing was not completed with a high total head existing near the flow centerline. However, examination of the total temperature distribution across the mixing tube exit shows a more linear profile at all flow conditions. Thus, it appears that if additional mixing tube lengths were added to obtain a linear temperature distribution, the velocity distribution would still be non-linear, as in the case of fully developed turbulent pipe flow. A decrease of total temperature near the wall is apparent which probably represents heat losses through the mixing section wall. The displacement of the measured temperature distribution from the theoretical is also an indication of heat losses. The amount of heat transfer appears to increase as the mass flow ratio decreases with a maximum displacement occuring at W_2/W_1 = 0. The above is as expected since the introduction of secondary mass flow at the circumference of the mixing tube entrance would effectively act as a heat barrier between the heated primary flow and the mixing tube wall.

Static pressure distributions along the mixing tube were also obtained and are shown in Figures 70 through 73. They indicate a gradual increase in the static pressure as the flow advances through the mixing tube. Shock and mixing losses are not apparent from the static pressure variation. It

should be noted that in the development of the theoretical equations the length of the mixing tube is not considered and there doesn't appear to be any simple method of doing so.

An indication of the effect of an increase in primary temperature upon ejector performance was indicated from experimental data in Section C. Figures 39 through 45 show these results while the dashed lines indicate the theoretical effect. It would appear that although the theory gives considerably better performance it still indicates quite accurately the relative effect of a change in primary temperature since the slopes of the curves are approximately the same. It must be pointed out that this agreement can not be expected to hold to an extreme primary temperature because of the assumption that $\gamma = 1.4$ regardless of the temperature.

IV. REFERENCES

1. Currey, Richard, <u>Experimental Study of Ejectors for Use in Exhausting Ram-Jet Test Burners</u>, UAC Report No. 32, (Meteor), January, 1949, (Confidential).

2. DeLeo, R. V. and Wood, R. D., <u>An Experimental Investigation of the Use of Hot Gas Ejectors for Boundary Layer Removal</u>, Part I, WADC TR 52-128, April, 1952.

3. Ellis, C. W., Holister, D. P., and Sargent, A. F., Jr., <u>Preliminary Investigation of Cooling-Air Ejector Performance at Pressure Ratios from 1 to 10</u>, NACA RM 51H21, October 17, 1951, (Confidential).

4. Elrod, H. G., Jr., <u>The Theory of Ejectors</u>, Journal of Applied Mechanics A-173, September 1945.

5. Fletcher, J. L., <u>Calculation of Airflow Through an Ejector - Operated Engine Cooling System for a Turbojet Powered Aircraft</u>, Douglas Aircraft Report No. SM-14020, May 10, 1951.

6. Flugel, Gustav, <u>The Design of Jet Pumps</u>, NACA TM No. 982, July 1941, (a translation from "Berechnung von Strahlapparaten", VDI-Forschungsheft 395, March-April 1939).

7. Fox, N. L., <u>Analytical Solutions for the Gross Thrust Change and Weight Flow Ratio Due to a Jet Ejector Pump</u>, Douglas Aircraft Company, Report SM-13881, December 1950.

8. Fox, N. L., <u>The Pumping Characteristics of Long Mixing Section Jet Pumps</u>, Douglas Aircraft Report No. SM-14385, September 5, 1952.

9. Huddleston, S.C., Wilsted, H. D., and Ellis, D. W., <u>Performance of Several Air Ejectors with Conical Mixing Sections and Small Secondary Flow Ratios</u>, NACA RM E8D23, July 19, 1948. (Restricted).

10. Jacobs, E. N., and Shoemaker, J. M., <u>Tests on Thrust Augmentors for Jet Propulsion</u>, NACA TN 431, September 1932.

11. Keenan, J. H., and Neumann, E. P., A Simple Air Ejector, Journal of Applied Mechanics, June 1942.

12. Keenan, J. H., Neumann, E. P. and Lustwerk, F., <u>An Investigation of Ejector Design by Analysis and Experiment</u>, M. I. T. Meteor Report No. 18, June 1948.

13. Kiselev, B. M., <u>Calculation of One-Dimensional Gas Flows</u>, Brown University Technical Report, No. F-TS-1209-1A (GDAM A9-T-27) (a translation) January 1949.

14. Klein, Harold, <u>The Thrust and Drag Penalties on a Jet Engine Installation Due to Cooling Flow</u>, Douglas Aircraft, Report No. SM-13862, November 7, 1950.

15. Manganiello, Eugene J. and Bogatsky, Donald, <u>An Experimental Investigation of Rectangular Exhaust-Gas Ejectors Applicable for Engine Cooling</u>, NACA ARR E4E31, May 1944 (E-224).

16. McElroy, G. E., <u>Design of Injectors for Low-Pressure Air Flow</u>, Bureau of Mines Technical Paper 678, 1945.

17. Schubauer, G. B., <u>Jet Propulsion with Special Reference to Thrust Augmentors</u>, NACA TN 442, January 1933.

18. Towle, H. C., Judd, F. V. H., <u>Ejectors for Cooling a Turbojet Installation</u>, Republic Aviation Corporation (no date).

19. Weeks, W. S., <u>The Air Injector for Auxiliary Ventilation Underground</u>, Engineering and Mining Journal, Vol. 138, No. 4, Page 196, April 1937.

20. Weinig, Fredrick, <u>Analysis of Thrust Augmentation Nozzle for High Velocity Drag Reduction</u>, Technical Report G5-USAF, Wright-Patterson Air Base, No. 99., No. F-TR-2212-ND (Confidential).

21. Wilder, J. C., <u>A Theoretical and Experimental Investigation of Jet-Augmentation</u>, Curtiss-Wright Corporation, Report No. BC-357-A-1. September, 1945.

22. Wilsted, N. D., Huddleston, S. C. and Ellis, C. W., <u>Effect of Temperature on Performance of Several Ejector Configurations</u>, NACA RM E9E16, June 13, 1949 (Restricted).

23. <u>Model Specification Engine</u>, Aircraft, Turbo-Jet J65-W-3, W. A. D. Spec. No. 884-A (by Curtiss-Wright Corp. - Wright Aeronautical Division), (Restricted), July 1949.

24. Anderson, K. G., <u>Investigation of Boundary Layer Control at High Subsonic Speeds</u>, AFTR No. 6344, January 1951.

APPENDIX A

DERIVATION OF THEORETICAL EJECTOR PERFORMANCE EQUATIONS

In the derivation of the following theoretical ejector performance equations the following assumptions have been made:

a. The flow is steady and one dimensional.

b. The perfect mixing of the two fluids is obtained within the mixing section. Both fluids are assumed to be air and perfect gases.

c. Mixing losses, nozzle losses and wall friction are neglected.

d. The walls of the mixing section are non-heat conducting and no phase or chemical change takes place within the section.

e. The adiabatic coefficient γ and gas constant R of the primary and secondary fluids are identical and independent of pressure and temperature.

f. The momentum and energy equations may be written over the boundaries of the mixing section without knowledge of the flow within the system.

The nomenclature and symbology used is defined in the Nomenclature section and Figure 4.

1.0 Basic Equations

The following basic equations have been used:

Continuity Equation

$$m = \rho V A \qquad (1.01)$$

Weight Flow Equation

$$W_3 = W_2 + W_1 \qquad (1.02)$$

Area Equation

$$A_3 = A_2 + A_1 \qquad \text{(for constant area mixing)} \qquad (1.03)$$

Momentum Equation

$$\left(m_1 V_1 + p_1 A_1\right) + \left(m_2 V_2 + p_2 A_2\right) = \left(m_3 V_3 + p_3 A_3\right) \qquad (1.04)$$

Energy Equation

$$m_1 T_1 + m_2 T_2 = m_3 T_3 \qquad (c_p = \text{constant}) \qquad (1.05)$$

2.0 Mixed Flow Velocity Relation

If we assume that the mixed flow at the exit of the mixing tube has expanded isentropically from an imaginary throat we may write from the continuity equation:

$$\theta(M^*) = \frac{A^*}{A} = \frac{\rho V}{\rho^* a^*} \qquad (2.01)$$

since

$$\rho V = \frac{m}{A}$$

where

$$m = \frac{W}{g}$$

and

$$\frac{\rho^*}{\rho_o} = \left(\frac{2}{\gamma+1}\right)^{\frac{1}{\gamma-1}}$$

$$\frac{a^*}{a_o} = \left(\frac{2}{\gamma+1}\right)^{\frac{1}{2}}$$

then

$$\theta(M^*) = \frac{W/g \cdot 1/A}{\rho_o \cdot \left(\frac{2}{\gamma+1}\right)^{\frac{1}{\gamma-1}} \left(\frac{2}{\gamma+1}\right)^{\frac{1}{2}} a_o}$$

since from the equations of state and energy

$$\rho_o = \frac{P}{RT} \qquad\qquad a_o = \sqrt{\gamma RT}$$

then

$$\theta(M^*) = \frac{R}{g\left(\frac{2}{\gamma+1}\right)^{\frac{1}{\gamma-1}} \left(\frac{2}{\gamma+1}\right)^{\frac{1}{2}} \left(\gamma R\right)^{\frac{1}{2}}} \cdot \frac{W\sqrt{T}}{PA}$$

$$\theta(M^*) = C \times \frac{W\sqrt{T}}{PA} \qquad\qquad (2.02)$$

where

$$C = f(\gamma, R, g) = 1.8745 \qquad\qquad \begin{array}{l} for \quad \gamma = 1.4 \\ R = 1715 \; ft^2/sec^2 \; {}^\circ F \\ g = 32.2 \; ft/sec^2 \end{array}$$

therefore

$$\theta(M_1^*) = C_1 \frac{W_1\sqrt{T_1}}{P_1 A_1}$$

$$\theta(M_2^*) = C_2 \frac{W_2\sqrt{T_2}}{P_2 A_2}$$

$$\theta(M_3^*) = C_3 \frac{W_3\sqrt{T_3}}{P_3 A_3}$$

If we write the ratio of mixing section area to primary nozzle area
we obtain

$$\frac{A_3}{A_1} = \frac{C_3 \dfrac{W_3\sqrt{T_3}}{P_3\, \theta(M_3^*)}}{C_1 \dfrac{W_1\sqrt{T_1}}{P_1\, \theta(M_1^*)}} \qquad\qquad (2.03)$$

Then from assumption (e)

$$C_1 = C_3$$

and

$$\frac{P_3 \, \theta(M_3{}^*)}{P_1 \, \theta(M_1{}^*)} = \frac{W_3}{W_1} \sqrt{\frac{T_3}{T_1}} \times \frac{A_1}{A_3}$$

Dividing both sides by P_a and noting that

$$\frac{W_3}{W_1} = \left(1 + \frac{W_2}{W_1}\right) \tag{2.04}$$

We obtain

$$\frac{P_3}{P_a} \, \theta(M_3{}^*) = \frac{P_1}{P_a} \, \theta(M_1{}^*) \left(1 + \frac{W_2}{W_1}\right) \sqrt{\frac{T_3}{T_1}} \, \frac{A_1}{A_3} \tag{2.05}$$

For flow in an ejector, without a diffuser at the exit of the mixing tube, we may assume that $p_3 \cong P_a$ for up to sonic exit velocities.

Then

$$\frac{P_3}{P_3} \, \theta(M_3{}^*) = f(M_3{}^*) = S(M_3{}^*)$$

Values of p_3/P_3 and $\theta(M_3^*)$ are tabulated in NACA TN 1428 for various values of M_3^*. A curve or table of the above function allows determination of the exit dimensionless velocity M_3^* or V_3/a_{3*}. In order to make use of the above equation the relationship between T_3 and T_1 must be found. This is quickly obtained from the energy equation as shown below:

$$m_3 \, T_3 = m_1 \, T_1 + m_2 \, T_2 \tag{1.05}$$

Then

$$\frac{T_3}{T_1} = \frac{\frac{W_2}{W_1}\frac{T_2}{T_1} + 1}{1 + \frac{W_2}{W_1}} \qquad\qquad (2.06)$$

In summary it may be seen that for the equation

$$S(M_3{}^*) = \frac{P_1}{P_a}\, \theta(M_1{}^*)\left(1 + \frac{W_2}{W_1}\right)\sqrt{\frac{T_3}{T_1}}\,\frac{A_1}{A_3} \qquad\qquad (2.07)$$

It is necessary to know or select the following parameters to obtain the exit dimensionless velocity:

$$A_1,\quad A_3,\quad \frac{T_1}{T_2},\quad \frac{P_1}{P_a},\quad \frac{W_2}{W_1},\quad M_1{}^* \text{ or } \theta(M_1{}^*)$$

The following facts should be noted concerning the above equation:

1. The primary nozzle exit velocity may be either subsonic, sonic, or supersonic.

2. The selected secondary quantities are W_2 and T_2.

3.0 Secondary Velocity Relation

The determination of the secondary flow entrance velocity is obtained by use of the momentum equation. We may define the momentum at any point by

$$(mV + pA) \qquad\qquad (3.01)$$

From the continuity equation (1.01)

$$m = \rho V A$$

$$(mV + pA) = m\left(V + \frac{p}{\rho V}\right)$$

and from the equations of state and energy

$$\frac{p}{\rho} = Rt = RT\left(1 - \frac{\gamma-1}{\gamma+1} M^{*2}\right)$$

where

$$\frac{R}{c_p} = \frac{\gamma-1}{\gamma} \quad \text{and} \quad c_p T = \frac{(\gamma+1)}{2(\gamma-1)} a_*^{\,2}$$

then

$$\frac{p}{\rho} = \frac{\gamma+1}{2\gamma} a_*^{\,2} \left(1 - \frac{\gamma-1}{\gamma+1} M^{*2}\right)$$

substituting

$$(mV + pA) = m\left[V + \frac{\gamma+1}{2\gamma} \frac{a_*^{\,2}}{V} \left(1 - \frac{\gamma-1}{\gamma+1} M^{*2}\right)\right]$$

$$= \frac{\gamma+1}{2\gamma} a_* m\left[\frac{2\gamma}{\gamma+1} M^* + \frac{1}{M^*} \left(1 - \frac{\gamma-1}{\gamma+1} M^{*2}\right)\right]$$

$$(mV + pA) = \frac{\gamma+1}{2\gamma} a_* m\left(M^* + \frac{1}{M^*}\right) \tag{3.02}$$

The conservation of momentum equation states

$$(m_1 V_1 + p_1 A_1) + (m_2 V_2 + p_2 A_2) = (m_3 V_3 + p_3 A_3) \qquad (1.04)$$

then from (3.02)

$$\left(\frac{\gamma+1}{2\gamma}\right) a_{*_1} m_1 \left(M_1^* + \frac{1}{M_1^*}\right) + \left(\frac{\gamma+1}{2\gamma}\right) a_{*_2} m_2 \left(M_2^* + \frac{1}{M_2^*}\right)$$

$$= \left(\frac{\gamma+1}{2\gamma}\right) a_{*_3} m_3 \left(M_3^* + \frac{1}{M_3^*}\right)$$

From our basic assumption (e) of $\gamma_1 = \gamma_2 = \gamma_3$ and dividing both sides by $m_1\, a_{*_1}$ we obtain

$$\frac{m_2\, a_{*_2}}{m_1\, a_{*_1}} \left(M_2^* + \frac{1}{M_2^*}\right) + \left(M_1^* + \frac{1}{M_1^*}\right) = \frac{m_3\, a_{*_3}}{m_1\, a_{*_1}} \left(M_3^* + \frac{1}{M_3^*}\right)$$

since $m = w/g$ and $a_* = \sqrt{2/(\gamma+1)}\, a_o$ where

$$a_o = \sqrt{\gamma R T} \qquad\qquad W_1 + W_2 = W_3$$

we arrive at

$$\frac{W_2}{W_1} \sqrt{\frac{T_2}{T_1}} \left(M_2^* + \frac{1}{M_2^*}\right) + \left(M_1^* + \frac{1}{M_1^*}\right) = \qquad (3.03)$$

$$\left(1 + \frac{W_2}{W_1}\right) \sqrt{\frac{T_3}{T_1}} \left(M_3^* + \frac{1}{M_3^*}\right)$$

The following facts should be noted concerning the above equation:

1. The ratio of T_3/T_1 is determined from the energy equation as shown in the previous section, equation (2.06).

2. The minimum value of $(M^* + 1/M^*)$ is equal to 2.0 and is obtained at $M^* = 1.0$.

3. To determine $(M_2^* + 1/M_2^*)$ we must know or select W_2/W_1, T_2/T_1, M_1^* and M_3^*.

4. To determine M_2^* we must either solve the quadratic equation or plot a curve of M_2^* versus $(M_2^* + 1/M_2^*)$. Both solutions are valid one being subsonic and the other supersonic velocities.

4.0 Secondary Pumping Pressure Relation

The only remaining unknown quantity in our analysis is the value of the secondary pumping pressure P_2. From section (2.0) we obtained the relation

$$A = C \frac{W\sqrt{T}}{P\theta(M^*)} \tag{2.02}$$

From this we may write

$$\frac{A_2}{A_1} = \frac{\dfrac{C_2 W_2 \sqrt{T_2}}{P_2 \theta(M_2^*)}}{\dfrac{C_1 W_1 \sqrt{T_1}}{P_1 \theta(M_1^*)}}$$

since $C_1 = C_2$ by assumption (e) and dividing the pressure by P_a we obtain

$$\frac{P_2}{P_a} = \frac{\dfrac{P_1}{P_a}\theta(M_1^*)\dfrac{W_2}{W_1}\sqrt{\dfrac{T_2}{T_1}}}{\dfrac{A_2}{A_1}\theta(M_2^*)} \tag{4.01}$$

where $\theta(M_2{}^*) = f(M_2{}^*)$

5.0 Ejector Pumping Pressure When $W_2/W_1 = 0$

It was found in Section 3 that the momentum at a particular point could be expressed as follows:

$$(mV + pA) = \frac{\gamma+1}{2\gamma} a_* m \left(M^* + \frac{1}{M^*}\right) \tag{3.02}$$

Writing the momentum ejector relationship as

$$\frac{\gamma+1}{2\gamma} a_* m_1 \left(M_1{}^* + \frac{1}{M_1{}^*}\right) + m_2 V_2 + p_2 A_2 = \frac{\gamma+1}{2\gamma} a_{*_1} m_3 \left(M_3{}^* + \frac{1}{M_3{}^*}\right)$$

for

$$\frac{W_2}{W_1} = 0 \qquad\qquad V_2 = 0$$

then

$$p_2 A_2 = \frac{\gamma+1}{2\gamma} a_{*_3} m_3 \left(M_3{}^* + \frac{1}{M_3{}^*}\right) - \frac{\gamma+1}{2\gamma} a_{*_1} m_1 \left(M_1{}^* + \frac{1}{M_1{}^*}\right) \tag{5.01}$$

but $\gamma_1 = \gamma_2 = \gamma_3$ by our original assumption (e) so

$$\frac{2\gamma}{\gamma+1} p_2 A_2 = a_{*_3} m_3 \left(M_3{}^* + \frac{1}{M_3{}^*}\right) - a_{*_1} m_1 \left(M_1{}^* + \frac{1}{M_1{}^*}\right)$$

dividing both sides by $a_{*_1} m_1$

$$\frac{\frac{2\gamma}{\gamma+1} p_2 A_2}{a_{*_1} m_1} = \frac{a_{*_3} m_3}{a_{*_1} m_1} \left(M_3^* + \frac{1}{M_3^*} \right) - \left(M_1^* + \frac{1}{M_1^*} \right)$$

From the isentropic functions we have previously found that

$$\frac{a_{*_3} m_3}{a_{*_1} m_1} = \left(1 + \frac{W_2}{W_1} \right) \sqrt{\frac{T_3}{T_1}}$$

For $W_2/W_1 = 0$ we found from the energy equation that $T_3/T_1 = 1.0$.
Therefore

$$\frac{\frac{2\gamma}{\gamma+1} p_2 A_2}{a_{*_1} m_1} = \left(M_3^* + \frac{1}{M_3^*} \right) - \left(M_1^* + \frac{1}{M_1^*} \right) \qquad (5.02)$$

Assuming that A_2 is the entrance ring area that the secondary flow must flow through to enter the mixing tube, we find that since $W_2 = 0$, $p_2 = P_2$.

Taking the term $a_{*_1} m_1$ we may write from the continuity relation and isentropic relationships:

$$m a_* = \rho_0 a_*^2 \left(1 - \frac{\gamma-1}{\gamma+1} M^{*2} \right)^{\frac{1}{\gamma-1}} M^* A \qquad (5.03)$$

The term $\rho_0 a_*^2$ using the energy equation and equation of state may be written

$$\frac{a_0^2}{a_*^2} = \frac{\gamma+1}{2} , \qquad a_0^2 = \gamma RT$$

$$P = \rho_0 RT$$

$$\rho_0 a_*^2 = \rho_0 a_0^2 \frac{2}{\gamma+1} = \rho_0 \gamma RT \frac{2}{\gamma+1}$$

$$\rho_0 a_*^2 = P \frac{2\gamma}{\gamma+1}$$

Then

$$ma_* = \frac{2\gamma}{\gamma+1} PA \left[M^* \left(1 - \frac{\gamma-1}{\gamma+1} M^{*2}\right)^{\frac{1}{\gamma-1}} \right] \qquad (5.04)$$

The term in the bracket is actually

$$M^* \frac{\rho}{\rho_0} = \frac{V}{a_*} \frac{\rho}{\rho_0}$$

Multipling and dividing by ρ_*

$$M^* \frac{\rho}{\rho_0} = \frac{\rho^*}{\rho_0} \cdot \frac{V\rho}{a_* \rho^*} = \frac{\rho^*}{\rho_0} \theta(M^*)$$

where

$$\theta(M^*) = \frac{A^*}{A} = \frac{V\rho}{a_* \rho^*}$$

We also know that

$$\frac{\rho_*}{\rho_0} = \left(\frac{2}{\gamma+1}\right)^{\frac{1}{\gamma-1}}$$

Then summing up we may obtain

$$m_1 a_{*_1} = \frac{2\gamma}{\gamma+1} P_1 A_1 \left(\frac{2}{\gamma+1}\right)^{\frac{1}{\gamma-1}} \theta(M_1^*) \qquad (5.05)$$

Inserting this in the original equation (5.02)

$$\frac{\frac{2\gamma}{\gamma+1}P_2 A_2}{\frac{2\gamma}{\gamma+1}P_1 A_1 \left(\frac{2}{\gamma+1}\right)^{\frac{1}{\gamma-1}}\theta(M_1{}^*)} = \left(M_3{}^* + \frac{1}{M_3{}^*}\right) - \left(M_1{}^* + \frac{1}{M_1{}^*}\right)$$

Since $\gamma_1 = \gamma_2 = \gamma_3$

and dividing by P_a

$$\frac{P_2}{P_a} = \left(\frac{2}{\gamma+1}\right)^{\frac{1}{\gamma-1}} \frac{P_1}{P_a} \frac{A_1}{A_2} \theta(M_1{}^*) \left[\left(M_3{}^* + \frac{1}{M_3{}^*}\right) - \left(M_1{}^* + \frac{1}{M_1{}^*}\right)\right] \quad (5.06)$$

The following facts should be noted concerning the above equation:

1. The value of P_2/P_a for $W_2/W_1 = 0$ is independent of the primary temperature T_1.

2. The value of $P_2/P_a = 0$ when $M_3{}^* = M_1{}^*$.

3. To determine P_2/P_a we must know or select P_1/P_a, $M_1{}^*$, $M_3{}^*$ and A_1/A_2.

6.0 Ejector - Jet Thrust Relation

It is assumed that the thrust of the primary jet and the ejected mixed flow may be given by:

Primary

$$F_j = m_1 V_1 + A_1 (p_1 - P_a) \quad \text{or}$$

$$F_j = m_1 V_1 + P_a A_1 \left(\frac{p_1}{P_a} - 1\right) \quad (6.01)$$

where

$$F_j{}' = m_1 V_1$$

Mixed Flow

$$F_e = m_3 V_3 + A_3 (p_3 - P_a)$$

but since $p_3 = P_a$ for up to sonic velocities

$$F_e = m_3 V_3 \tag{6.02}$$

Therefore the ejector-jet thrust ratio is

$$\frac{F_e}{F_j} = \frac{m_3 V_3}{m_1 V_1 + P_a A_1 \left(\frac{p_1}{P_a} - 1\right)}$$

or

$$\frac{F_e}{F_j} = \frac{\dfrac{m_3 V_3}{m_1 V_1}}{1 + \dfrac{P_a A_1 \left(\frac{p_1}{P_a} - 1\right)}{m_1 V_1}} \tag{6.03}$$

For

$$P_1 \leq 1.89 \, P_a \qquad p_1 = P_a \quad and \quad F_j = F_j{}'$$

then

$$\frac{F_e}{F_j} = \frac{F_e}{F_j{}'} = \frac{m_3 V_3}{m_1 V_1} \tag{6.04}$$

From the basic equation and several isentropic relations we know:

$$m_3 = \frac{W_1 + W_2}{g} \qquad\qquad m_1 = \frac{W_1}{g}$$

$$V_3 = M_3{}^* a_{*3} \qquad\qquad V_1 = M_1{}^* a_{*1}$$

$$\frac{a_*}{a_o} = \sqrt{\frac{2}{\gamma+1}} \qquad\qquad a_o = \sqrt{\gamma R T}$$

Then from equation (6.04) we write

$$\frac{F_e}{F_j'} = \left(1 + \frac{W_2}{W_1}\right) \sqrt{\frac{T_3}{T_1}} \frac{M_3^*}{M_1^*} \qquad for \qquad \frac{P_1}{P_a} \leq 1.89 \qquad (6.05)$$
$$and \qquad \gamma_1 = \gamma_3$$

where T_3/T_1 and M_3^* may be determined from equations 2.06 and 2.07. M_1^* may be found from $p_1/P_1 = f(M_1^*)$.

The term in our original thrust ratio equation 6.03

$$\frac{P_a A_1 \left(\frac{p_1}{P_a} - 1\right)}{m_1 V_1} \neq 0 \qquad when \qquad \frac{P_1}{P_a} > 1.89$$

where $m_1 V_1 = m_1 a_{1*} M_1^*$.

In Section 5 we had found that

$$m_1 a_{*_1} = \frac{2\gamma}{\gamma+1} P_1 A_1 \left(\frac{2}{\gamma+1}\right)^{\frac{1}{\gamma-1}} \theta(M_1^*) \qquad (5.04)$$

Therefore

$$m_1 a_{*_1} M_1^* = \frac{2\gamma}{\gamma+1} P_1 A_1 \left(\frac{2}{\gamma+1}\right)^{\frac{1}{\gamma-1}} \theta(M_1^*) M_1^*$$

or

$$\frac{P_a A_1 \left(\frac{p_1}{P_a} - 1\right)}{m_1 V_1} = \frac{P_a A_1 \left(\frac{p_1}{P_a} - 1\right)}{\frac{2\gamma}{\gamma+1} P_1 A_1 \left(\frac{2}{\gamma+1}\right)^{\frac{1}{\gamma-1}} \theta(M_1^*) M_1^*}$$

$\div$ top and bottom of right side by P_1

$$\frac{P_a A_1 \left(\frac{P_1}{P_a} - 1 \right)}{m_1 V_1} = \frac{\left(\frac{P_1}{P_1} - \frac{P_a}{P_1} \right)}{\left(\frac{2\gamma}{\gamma+1} \right) \left(\frac{2}{\gamma+1} \right)^{\frac{1}{\gamma-1}} \theta(M_1{}^*) M_1{}^*} \quad (6.06)$$

Then

$$\frac{F_e}{F_j} = \frac{\left(1 + \frac{W_2}{W_1} \right) \sqrt{\frac{T_3}{T_1}} \frac{M_3{}^*}{M_1{}^*}}{1 + \frac{\left(\frac{P_1}{P_1} - \frac{P_a}{P_1} \right)}{\left(\frac{2\gamma}{\gamma+1} \right) \left(\frac{2}{\gamma+1} \right)^{\frac{1}{\gamma-1}} \theta(M_1{}^*) M_1{}^*}} \quad (6.07)$$

It should be noted that for conditions up to sonic in the primary nozzle $P_1 = P_a$.

For a convergent primary nozzle and $p_1/P_a > 1.89$ with $\gamma_1 = 1.4$ then

$$M_1{}^* = 1.0 \quad and \quad \theta(M_1{}^*) = 1.0$$

$$\frac{F_e}{F_j} = \frac{\frac{M_3 V_3}{M_1 V_1}}{1 + \frac{\left(0.528 - \frac{P_a}{P_1} \right)}{0.7396}} \quad (6.08)$$

The following facts should be noted concerning the above equations:

1. The equation is valid only for a convergent nozzle.

2. The selected quantities are W_2/W_1, A_1/A_3, T_1/T_2, P_1/P_a.

3. The velocity at the exit of the mixing tube is determined from equation 2.07.

A P P E N D I X B

SOLUTION OF A SIMPLE EJECTOR DESIGN PROBLEM

The primary purpose of this phase of ejector study has been to provide experimental ejector data for engineering design purposes. The program has been tailored to cover the operational range of a modern turbo-jet engine since it may serve as a source of inductive power for aircraft boundary layer control applications. The use of data for the solution of a simple ejector design problem is given below.

<u>Given:</u> Boundary layer removal by suction is to be used on a turbo-jet aircraft during landing. The following operational data is available.

A. <u>Engine Test Data</u> (obtained from reference 23)

<u>Flight Condition</u>	<u>Landing</u>
Percent military power	30
Thrust, F_j, (lb)	2170
Turbine discharge total pressure, $(P_1/P_A)_t$	1.30
Turbine discharge total temperature, $(T_1/T_A)_t$	2.10
Compressor discharge total pressure $(P_1/P_A)_c$	3.80
Compressor discharge total temperature $(T_1/T_A)_c$	1.60
Engine mass flow, W_1 (lb/sec)	70

B. <u>Boundary Layer Removal Requirements</u> (assumed)

Required mass flow to be removed by suction, W_2, (lb/sec)	7.0
Required suction pressure ratio, P_2/P_a	0.80

C. <u>Atmospheric Conditions</u> (assumed)

$P_a = 14.7$ psia
$T_a = 520°R$

<u>To Determine</u>: Ejector configurations to satisfy boundary layer removal requirements.

A. <u>Installation Using Engine Exhaust Jet with a Tail Pipe Ejector</u>

From the above conditions the ejector operation may be defined as follows:

P_1/P_a	T_1/T_a	W_2/W_1	(W_2/W_1)	P_2/P_a
1.30	2.10	0.100	0.126	0.80

Since the ejector data available in this report is at $T_1/T_a = 3.32$ the required mass flow ratio was corrected to this condition as follows:

$$(W_2/W_1)_c = (W_2/W_1)(3.32/T_1/T_a)^{1/2}$$

As mentioned in section III-C, this will be a conservative correction in this case since the corrected required weight flow ratio will probably be slightly high. In order to determine the desired ejector geometry weight flow ratio and thrust ratio should be plotted versus area ratio as shown below. The data was obtained from the original data plots of Figures 8 through 23. In all cases interpolation was necessary because the data was not available at the desired primary compression ratio, $P_1/P_a = 1.30$. From the graph the following design conditions are apparent:

$$A_3/A_1 = 2.72, \quad F_e/F_j = 0.737$$

PREDICTED EJECTOR PERFORMANCE
(WITHOUT DIFFUSER)

$T_1/T_a = 3.32 \quad P_1/P_a = 1.30 \quad P_2/P_a = 0.80$
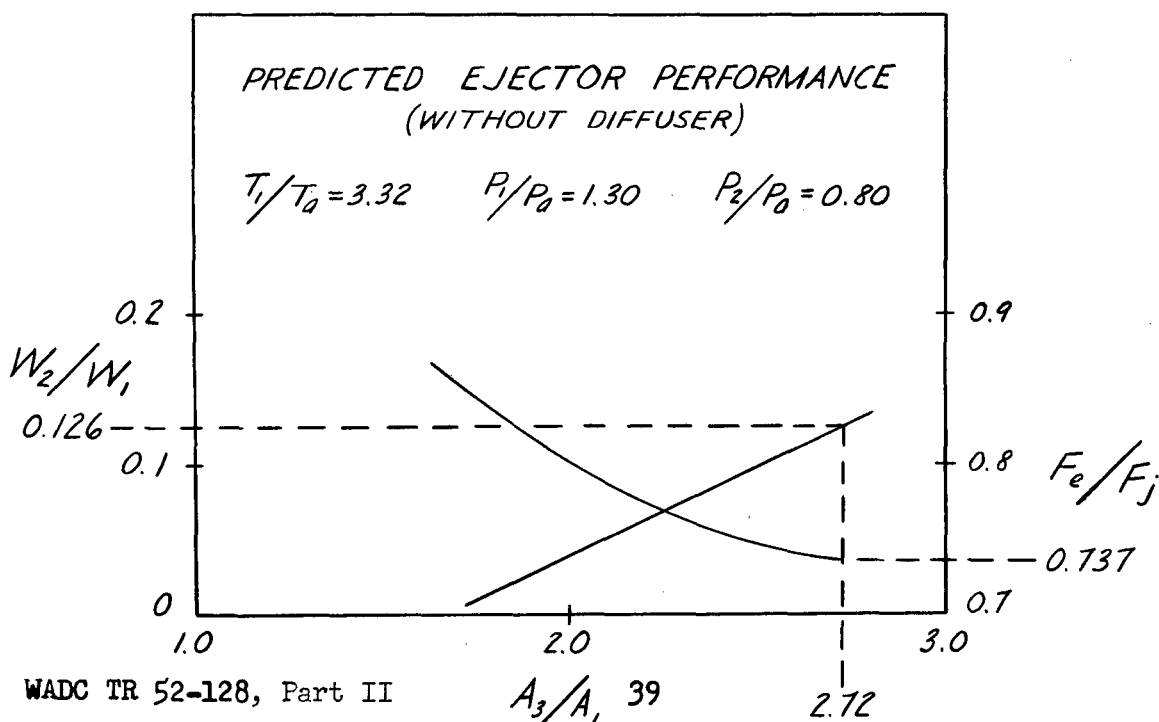
B. **Installation Using Engine Compressor Air Bleed and Auxiliary Ejector**
    With Diffuser

The ejector design operating conditions may be determined from the given engine characteristics and boundary layer removal requirements.

P_1/P_a	T_1/T_a	W_1 (lb/sec)	P_2/P_a
3.80	1.60	7.0	0.80

From the data plotted below at P_1/P_a = 3.80, (A_3/A_1) opt. = 9.75 with W_2/W_1 = 2.45. In order to correct the mass flow ratio to T_1/T_a = 1.60 the following may be used:

$$(W_2/W_1)_c = (W_2/W_1) \left[(T_1/T_a)/3.32 \right]^{1/2} = 2.45 \times .694 = 1.70$$

The compressor air bleed weight flow is then 7.0/1.7 = 4.11 lb/sec. By use of the method outlined in reference 23, the jet thrust ratio was calculated at 0.835.

PREDICTED EJECTOR PERFORMANCE
(WITH DIFFUSER)
T_1/T_a = 1.60 P_1/P_a = 3.80 P_2/P_a = 0.80
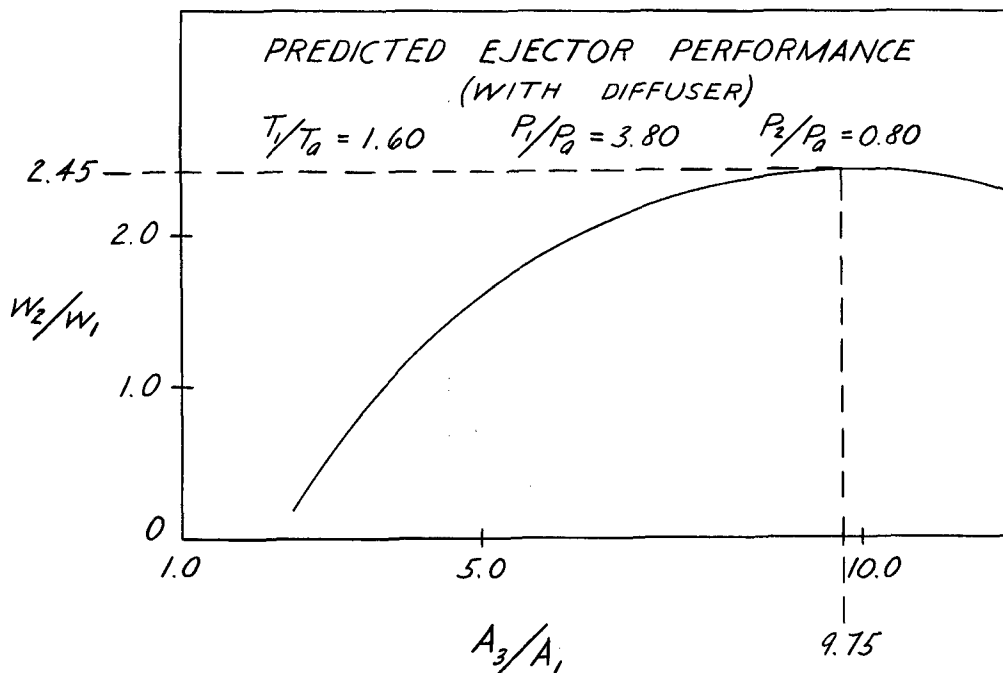
To determine the size of the primary jet required it must be remembered that it exhausts at the mixing tube entrance where $p_2 \leqq 0.8\ P_a$ and $p_1 = p_2$ (unless the primary nozzle is choked).

Thus:

$$\frac{p_1}{P_1} \leqq \frac{0.8\ P_a}{1.3\ P_a} \leqq 0.614$$

$$1.00 \geqq M_1{}^* \geqq 0.883$$

$$1.00 \geqq \frac{A_1{}^*}{A} \geqq 0.983$$

If it is assumed that $p_2 = P_2 = p_1 = 0.8\ P_a$, then by use of equation 2.02 of Appendix A

$$A_1 = \frac{1.87\ W_1\ (T_1)^{\frac{1}{2}}}{\dfrac{A_1{}^*}{A_1}\ P_1} = \frac{1.87 \times 4.11\ (520 \times 1.60)^{\frac{1}{2}}}{0.983 \times 14.7 \times 1.3} = 11.86\ in^2$$

$$D_1 = \left(11.86 \times \frac{4}{\pi}\right)^{\frac{1}{2}} = 3.88\ in$$

Using equation 2.02 of Appendix A for the secondary flow at the mixing tube entrance (constant area mixing)

$$A_2{}^* = \frac{1.87\ W_2\ (T_2)^{\frac{1}{2}}}{P_2} = \frac{1.87 \times 7.0\ (520)^{\frac{1}{2}}}{0.8 \times 14.7} = 25.3\ in^2$$

Then

$$\frac{A_2{}^*}{A_2} = \frac{A_2{}^*}{\left(\dfrac{A_3}{A_1} - 1\right) A_1} = \frac{25.3}{(9.75 - 1)\ A_1} = \frac{25.3}{8.75 \times 11.86}$$

$$= 0.244$$

thus

$$M_2{}^* = 0.143, \qquad \frac{p_2}{P_2} \cong 0.986$$

So the assumption of $p_2 \cong P_2$ has been justified. In certain applications, however, the assumption that $p_2 \cong P_2$ may not be valid so that a second approximation for the value of p_1 based on the calculated M_2^* may be necessary.

SCHEMATIC DRAWING
OF
HOT GAS EJECTOR INSTALLATION

FIGURE - 1
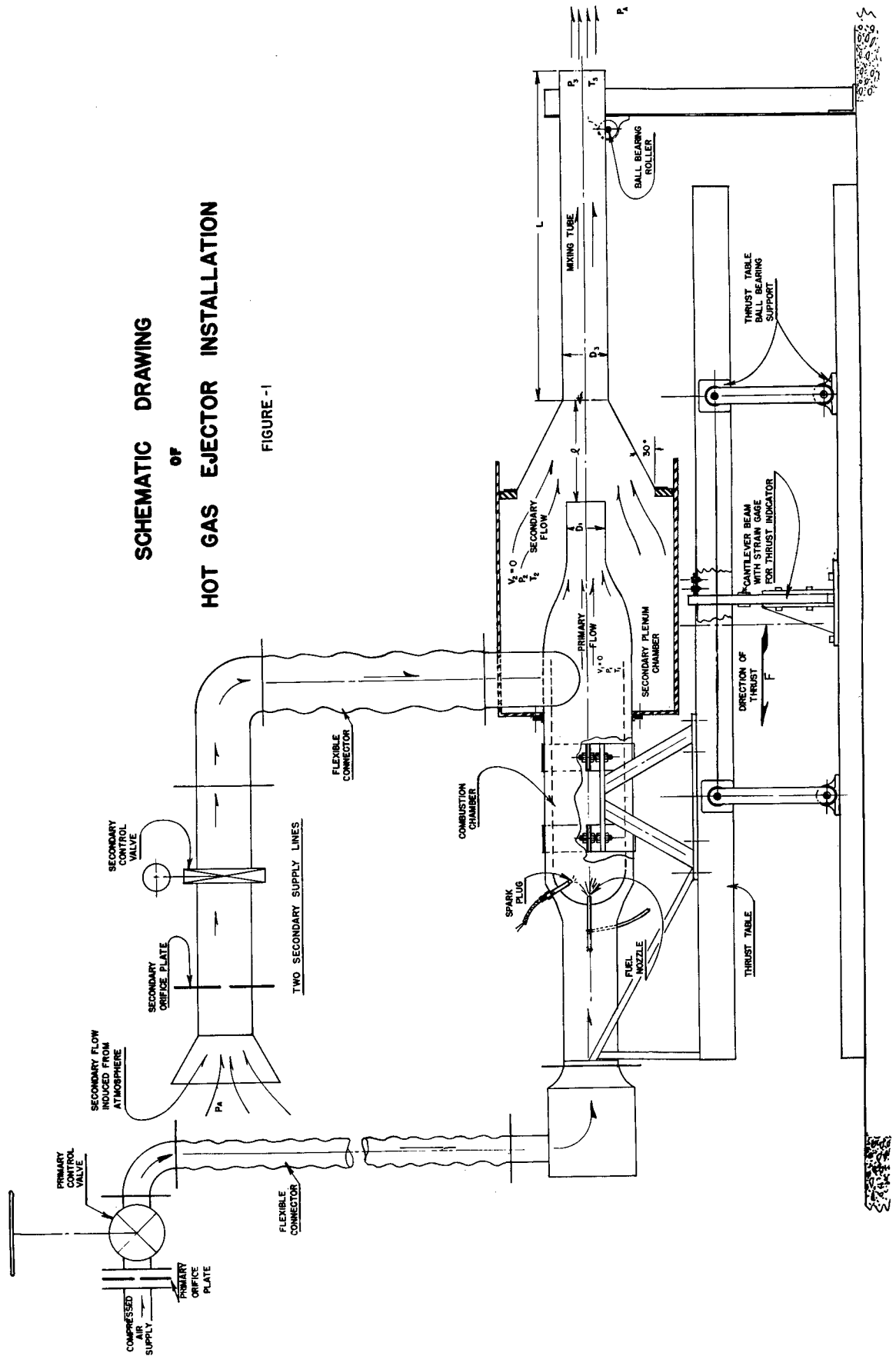
FIGURE- 2

COMBUSTION TEST FACILITY
INSTRUMENTATION AND CONTROL ROOM

COMBUSTION PRESSURE
SAFETY CUTOFF

PRIMARY AIR
CONTROL VALVE
HIGH PRESSURE
FUEL GAGE
SECONDARY VACUUM
GAGE
FUEL SUPPLY
PRESSURE GAGE
COMBUSTION CHAMBER
ENTRANCE PRESSURE GAGE
PRIMARY PRESSURE GAGE
HIGH TEMPERATURE
SAFETY CUTOFF
IGNITION SWITCH
SECONDARY CONTROL
VALVES

THRUST CALIBRATION
INSTRUMENT
TEMPERATURE MEASURING
INSTRUMENT
PRIMARY SUPPLY
PRESSURE GAGE
THRUST INDICATOR
SECONDARY PRESSURE
GAGE
PRIMARY MASS FLOW
MANOMETER
SECONDARY MASS FLOW
MANOMETER

FIGURE-3

HOT GAS EJECTOR

INSTALLATION

SECONDARY FLOW ENTRANCE LINES

PRIMARY FLOW ENTRANCE LINE

COMBUSTION CHAMBER

THRUST CANTILEVER BEAM

DIFFUSER

THRUST TABLE

ENTRANCE CONE AND MIXING TUBE
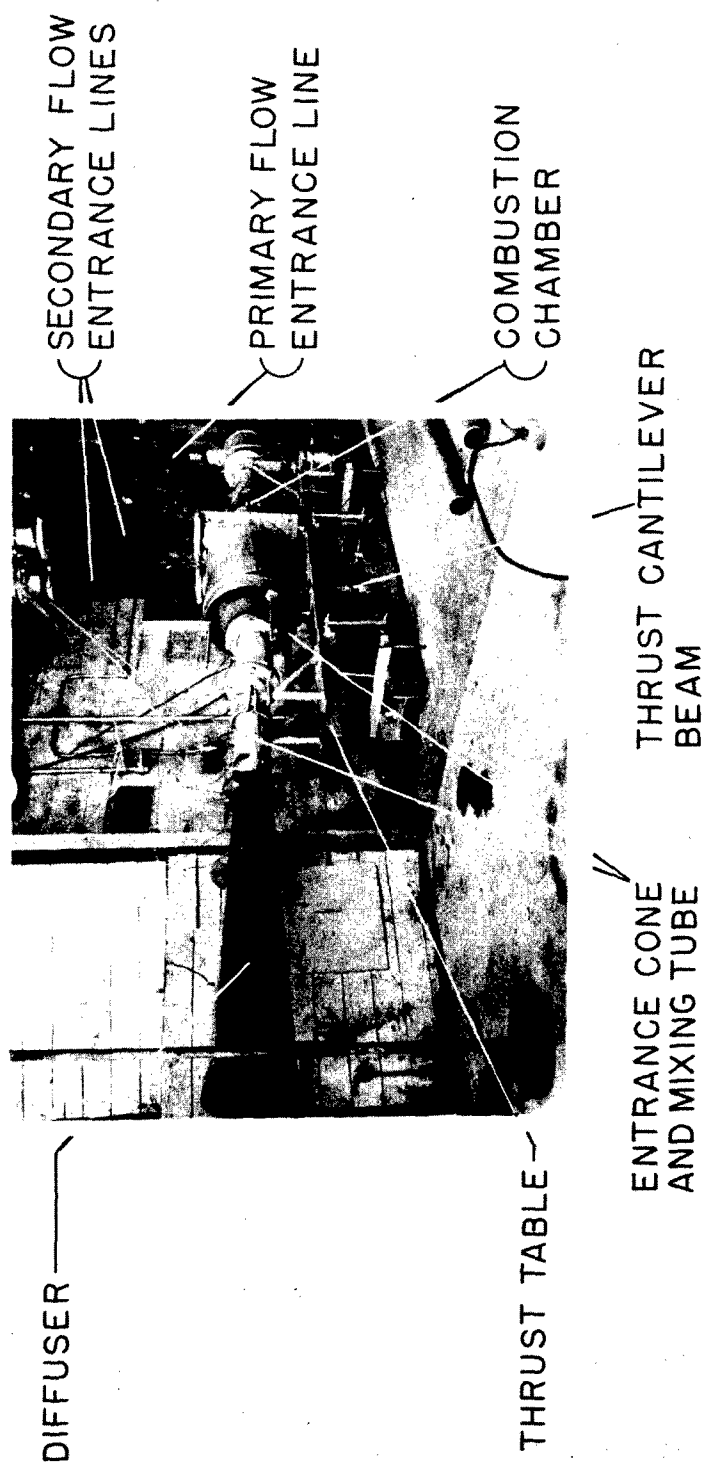
FIGURE 4

HOT GAS EJECTOR NOMENCLATURE
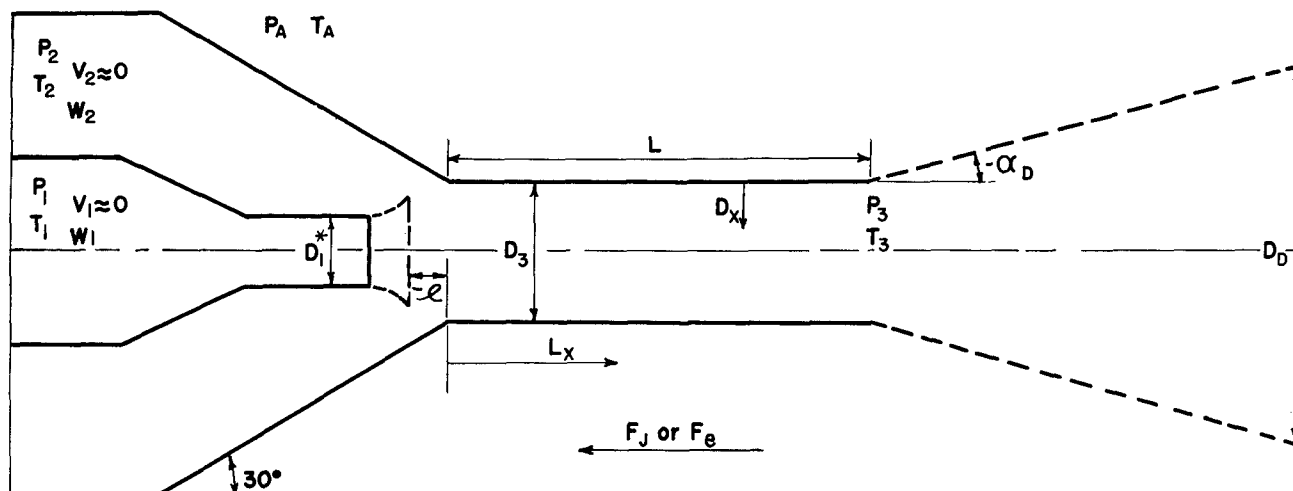
SYMBOLS

A — CROSS-SECTIONAL AREA OF CONFIGURATION
D — DIAMETER OF CONFIGURATION
F — THRUST
ℓ — PRIMARY JET LOCATION
L — LENGTH OF MIXING TUBE OR PRIMARY NOZZLE
P — STAGNATION PRESSURE
p — STATIC PRESSURE
T — STAGNATION TEMPERATURE
t — STATIC TEMPERATURE
V — VELOCITY OF FLOW
W — WEIGHT FLOW
α — GEOMETRIC ANGLE

SUBSCRIPTS

1 — PRIMARY FLOW
2 — SECONDARY FLOW
3 — MIXED FLOW
A — AMBIENT CONDITIONS
D — DIFFUSER EXIT CONDITIONS
X — DISTANCE ALONG LENGTH OR ACROSS DIAMETER
e — EJECTOR APPARATUS
J — PRIMARY APPARATUS
* — PRIMARY THROAT CONDITIONS

*AND 1 ARE EQUAL FOR CONVERGENT NOZZLE

PRIMARY MASS FLOW
FIGURE- 5
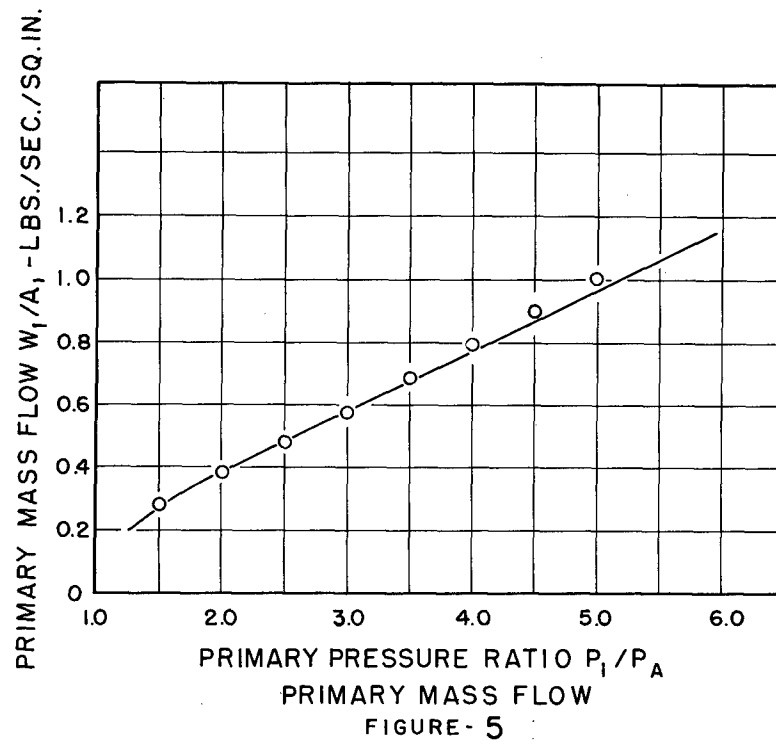
PRIMARY MASS FLOW AND THRUST

O   EXPERIMENTAL VALUES
—   THEORETICAL CURVE
P_A=29.92" Hg. T_I=1200°F
A_I= 11.7 SQ. IN.

PRIMARY THRUST
FIGURE- 6
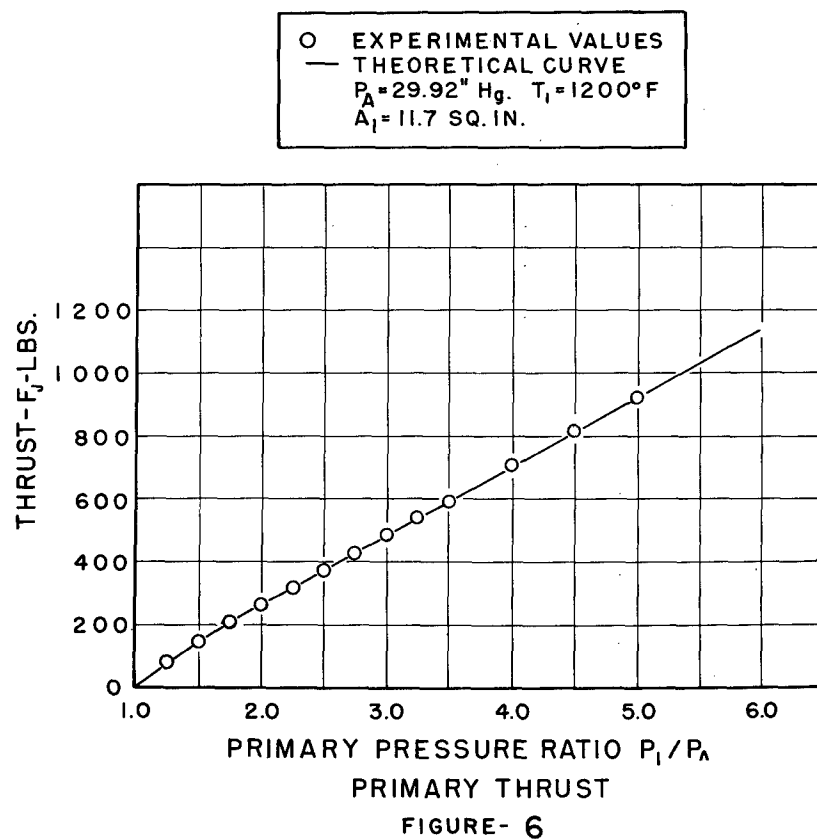
FIGURE- 7 - 8

EJECTOR PERFORMANCE
(WITHOUT DIFFUSER)
$A_3/A_1 = 1.21$

SYMBOLS- P_1/P_A		T_1/T_A = 3.32
△ = 1.25	⬭ = 2.00	D_3 = 4.25"
◇ = 1.50	◈ = 2.25	L = 7.5 D_3
◊ = 1.75	◠ = 2.50	$\mathfrak{a}$ = 0
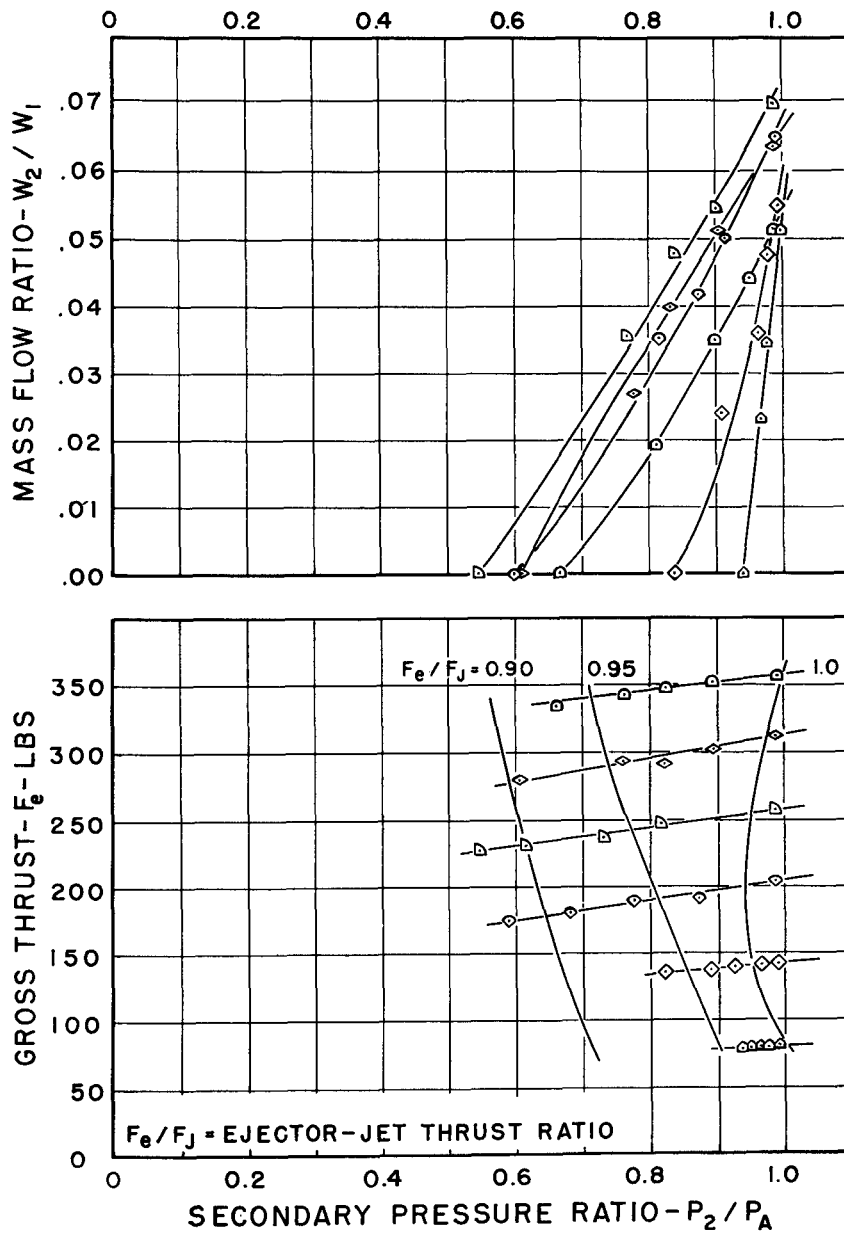
FIGURE- 9 - 10

EJECTOR PERFORMANCE
(WITHOUT DIFFUSER)
$A_3 / A_1 = 1.41$

SYMBOLS- P_1 / P_A		
△ = 1.25	◻ = 2.50	$T_1 / T_A = 3.32$
◇ = 1.50	▽ = 2.75	$D_3 = 4.5"$
◇ = 1.75	◿ = 3.00	$L = 7.5 D_3$
◻ = 2.00	◇ = 3.25	$\ell = 0$

$F_e / F_J = 0.80$

0.85   0.90   0.95

1.0

F_e / F_J = EJECTOR-JET THRUST RATIO

SECONDARY PRESSURE RATIO- P_2 / P_A

MASS FLOW RATIO- W_2 / W_1

GROSS THRUST- F_e - LBS
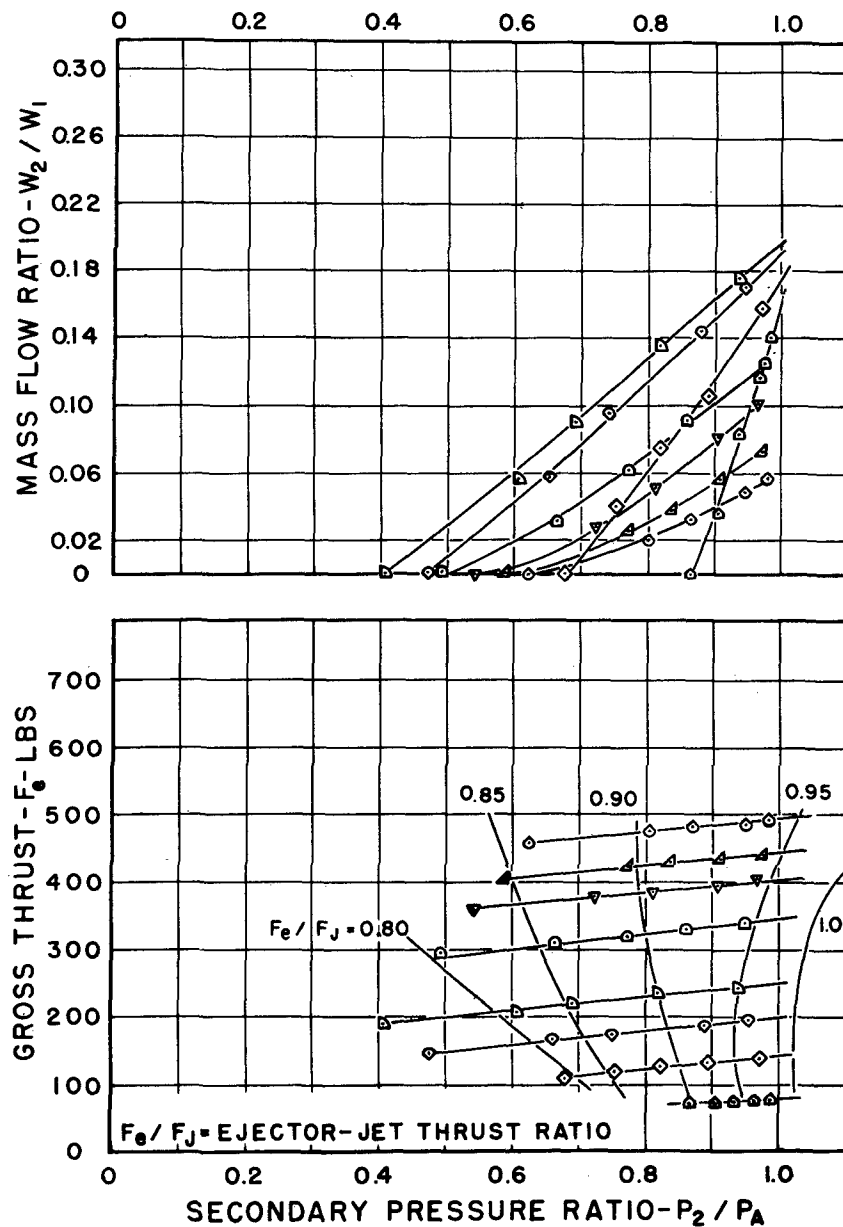
FIGURE- II - I2

EJECTOR PERFORMANCE
(WITHOUT DIFFUSER)
$A_3/A_1 = 1.72$

SYMBOLS- P_1/P_A		$T_1/T_A = 3.32$
△ = 1.25	◨ = 2.50	$D_3 = 5.0"$
◇ = 1.50	▽ = 2.75	$L = 7.5 D_3$
◇ = 1.75	◁ = 3.00	
◻ = 2.00	◌ = 3.25	$\mathbf{\mathcal{L}} = 0$
◇ = 2.25		

WADC 52- 128, Part II   50

FIGURE- 13 - 14

EJECTOR PERFORMANCE
(WITHOUT DIFFUSER)
$A_3/A_1 = 2.10$

SYMBOLS- P_1/P_A		$T_1/T_A = 3.32$
$\diamond$ = 1.50	$\bigcirc$ = 2.50	$D_3 = 5.5"$
$\triangledown$ = 1.75	$\triangledown$ = 2.75	$L = 7.5D_3$
$\square$ = 2.00	$\triangleleft$ = 3.00	
$\diamondsuit$ = 2.25	$\triangle$ = 3.50	$\mathit{l} = 0$

SECONDARY PRESSURE RATIO- P_2/P_A

F_e/F_J = EJECTOR-JET THRUST RATIO
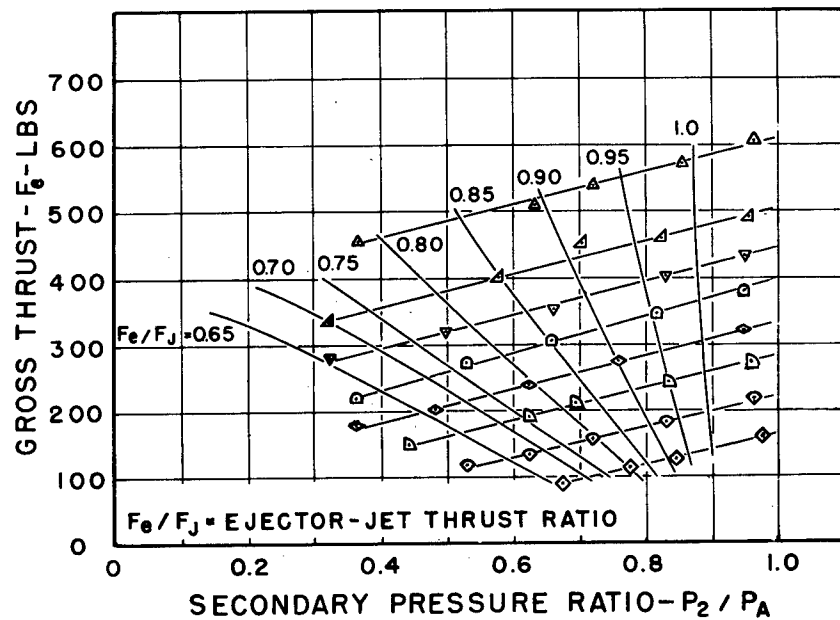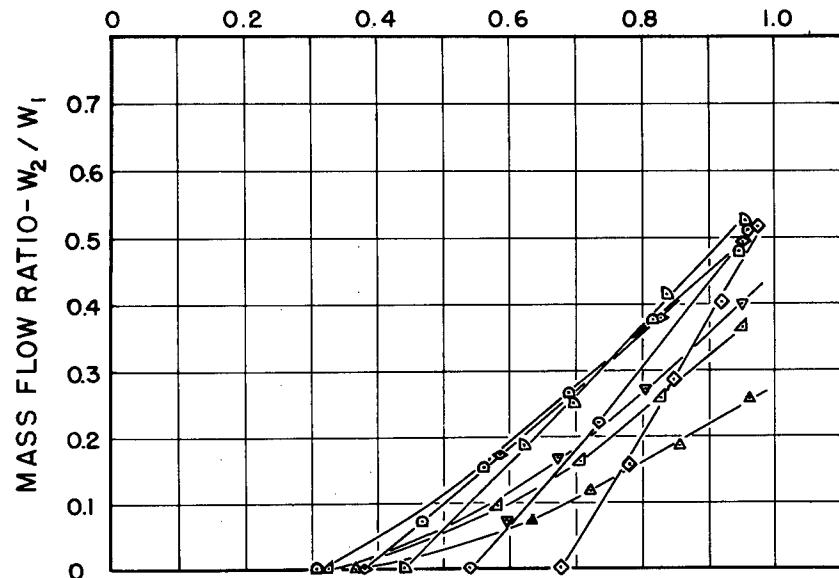
FIGURE- 15 - 16

EJECTOR PERFORMANCE

(WITHOUT DIFFUSER)

$A_3/A_1 = 2.48$

SYMBOLS P_1/P_A		$T_1/T_A = 3.32$
◇ = 1.50	◿ = 3.00	$D_3 = 6.0''$
◻ = 2.00	◊ = 4.00	$L = 7.5D_3$
◠ = 2.50		◠ = 0

WADC 52-128, Part II   52
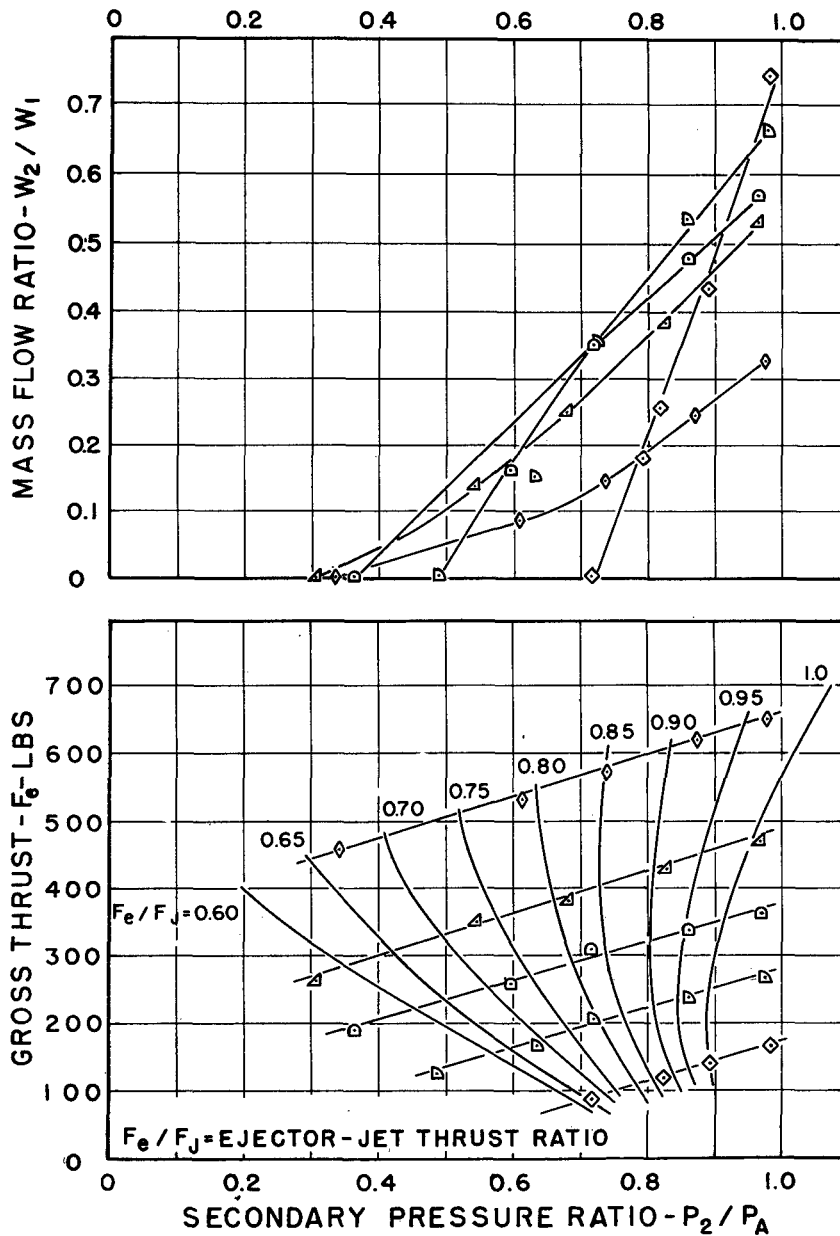
FIGURE-17-18

EJECTOR PERFORMANCE

(WITHOUT DIFFUSER)

$A_3/A_1 = 3.39$

SYMBOLS- P_1/P_A		$T_1/T_A = 3.32$
◇ = 1.50	△ = 3.50	$D_3 = 7.1''$
▷ = 2.00	◇ = 4.00	$L = 7.5 D_3$
◁ = 3.00	□ = 4.50	$\Omega = 0$
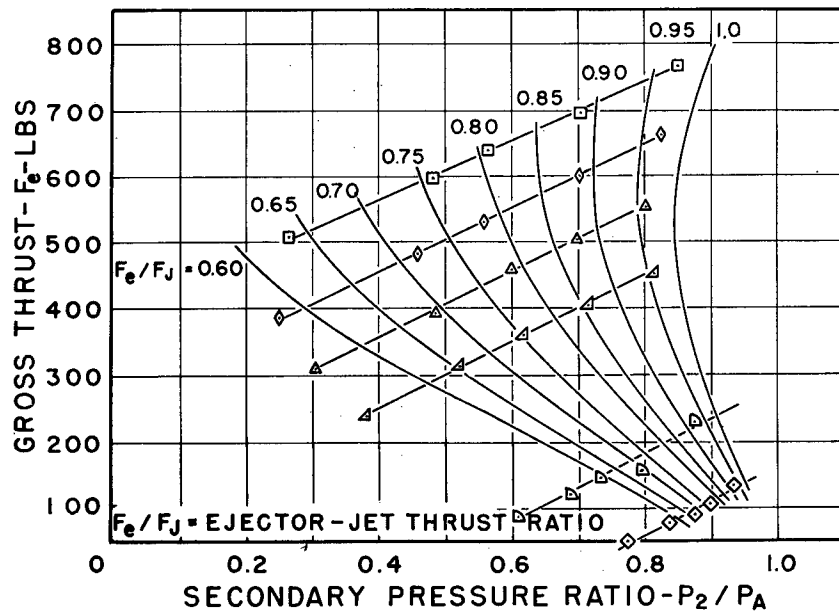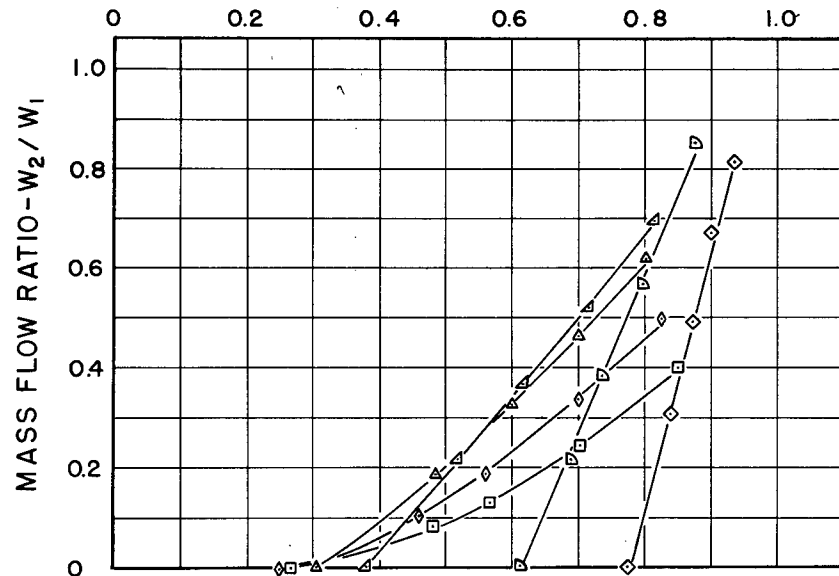
FIGURE- 19 - 20

EJECTOR PERFORMANCE
(WITHOUT DIFFUSER)
$A_3/A_1 = 4.30$

SYMBOLS- P_i/P_A		$T_i/T_A = 3.16$
$\diamond = 1.50$	$\triangle = 3.00$	$D_3 = 8.0"$
$\square = 2.00$	$\diamondsuit = 4.00$	$L = 7.5 D_3$
$\square = 2.50$		$\mathcal{a} = 0$
$\bigcirc = 5.00, T_i/T_A = 2.68$		
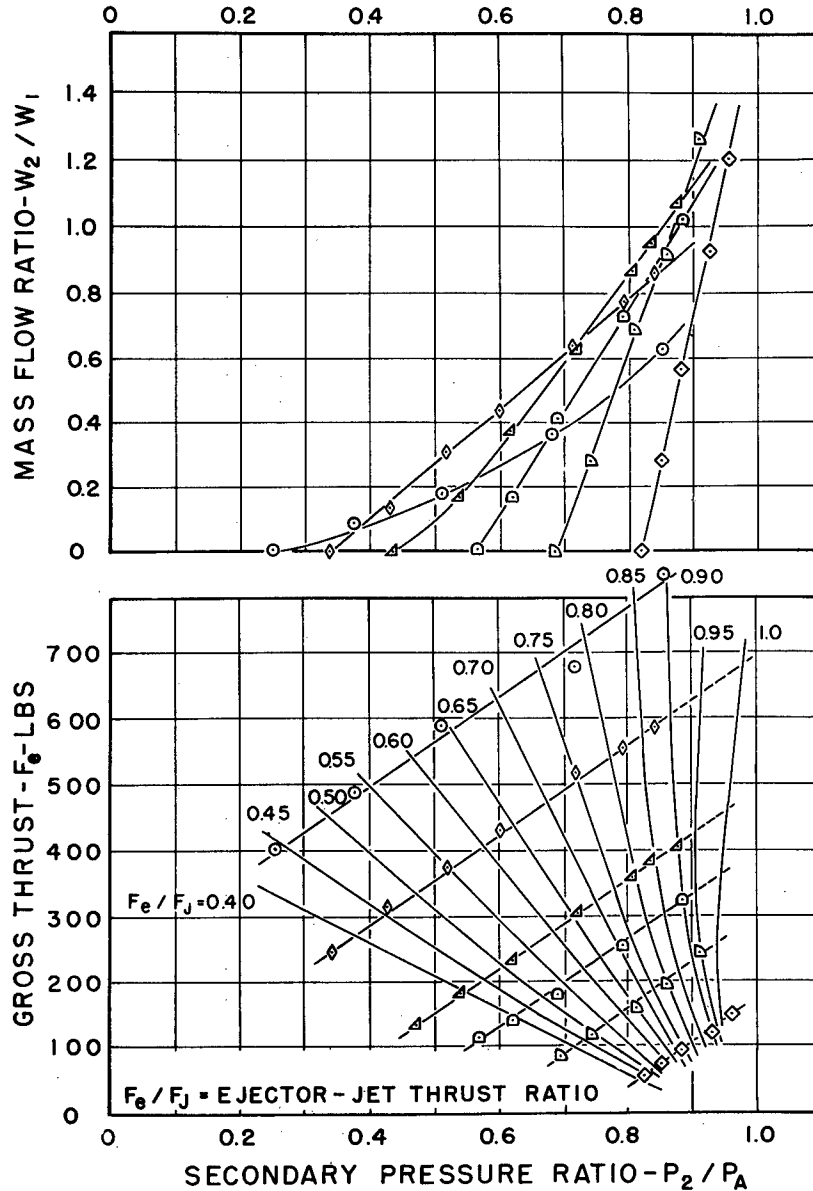
FIGURE-21-22

EJECTOR PERFORMANCE
(WITHOUT DIFFUSER)
$A_3/A_1 = 6.00$

SYMBOLS-P_1/P_A		$T_1/T_A = 3.32$
$\diamond$ = 1.50	$\triangle$ = 3.00	$D_3 = 9.45''$
$\square$ = 2.00	$\diamondsuit$ = 4.00	$L = 7.5 D_3$
$\bigcirc$ = 5.00	$T_1/T_A = 2.90$	$\mathit{\Omega} = 0$
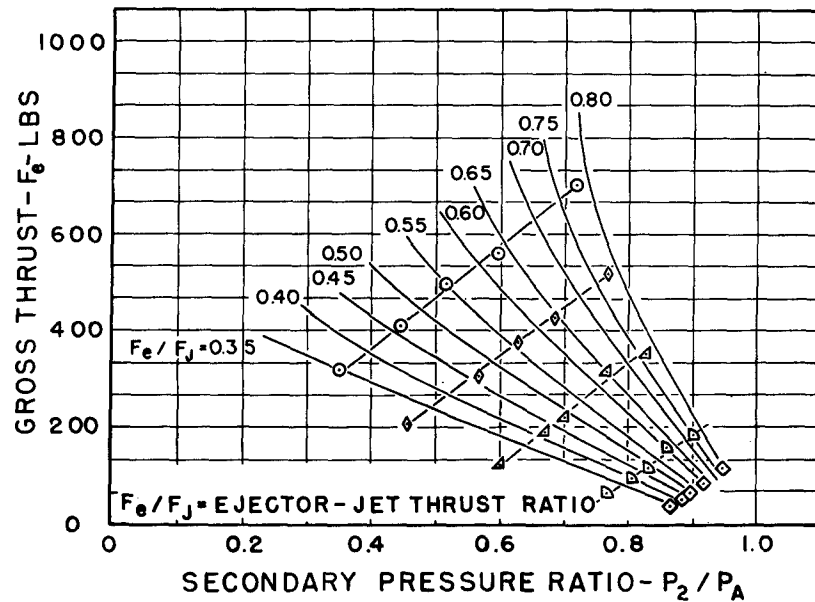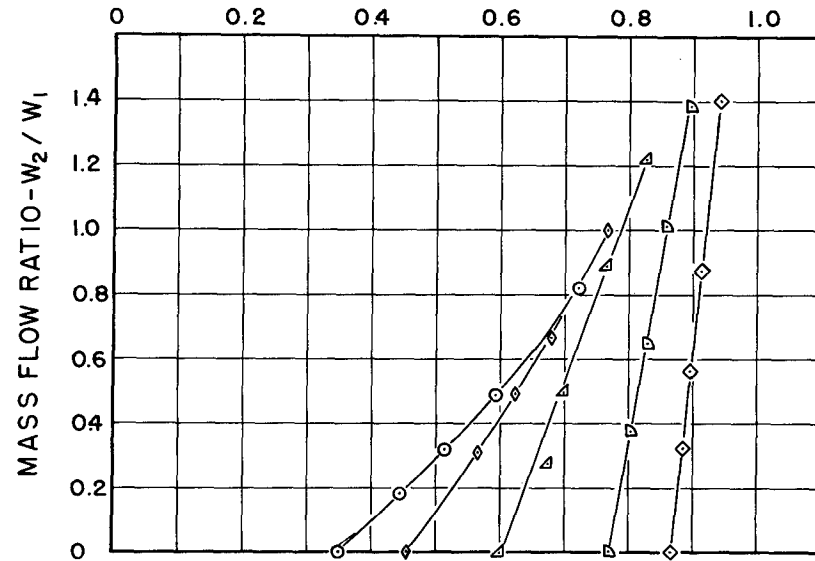
OPTIMUM PRIMARY PRESSURE RATIO
(WITH & WITHOUT DIFFUSER)

FIGURE- 24

$(A_3/A_1 = 2.48)$

$(A_3/A_1 = 1.72)$

FIGURE- 23

$(A_3/A_1 = 4.30)$

FIGURE- 25

OPTIMUM EJECTOR AREA RATIO
(WITHOUT DIFFUSER)

FIGURE-28

$P_2/P_A = .80$, .75, .70, .65, .60, .55, .50, .45, .40, .35

MASS FLOW RATIO W_2/W_1

EJECTOR AREA RATIO — A_3/A_1

$P_1/P_A = 3.00$

FIGURE-29

0.75, 0.70, 0.65, 0.60, 0.55, 0.50, 0.45, 0.40, 0.35

$P_2/P_A = 0.80$

MASS FLOW RATIO W_2/W_1
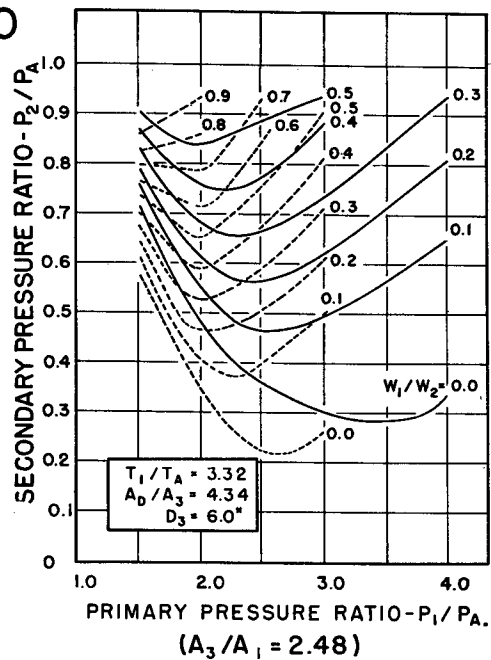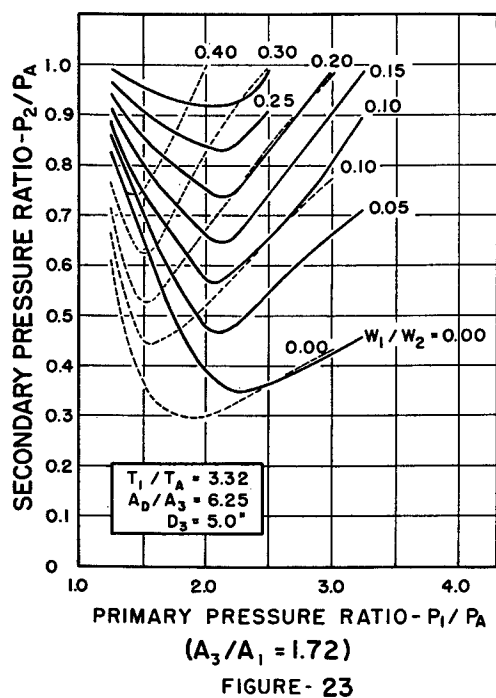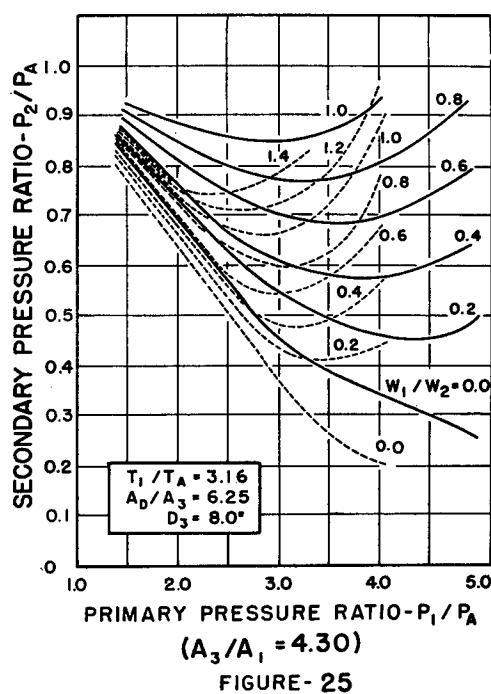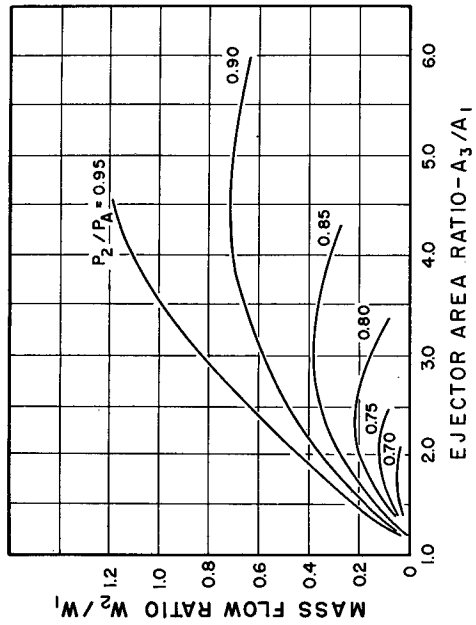
EJECTOR AREA RATIO — A_3/A_1

$P_1/P_A = 4.00$

A_3/A_1	
1.21	2.48
1.41	3.39
1.72	4.30
2.10	6.00

$T_1/T_A = 3.32$	
$L = 7.5 D_3$	
$\alpha = 0$	

FIGURE-26

$P_2/P_A = 0.95$, 0.90, 0.85, 0.80, 0.75, 0.70

MASS FLOW RATIO W_2/W_1

EJECTOR AREA RATIO — A_3/A_1

$P_1/P_A = 1.50$

FIGURE-27

$P_2/P_A = 0.95$, 0.90, 0.85, 0.80, 0.75, 0.70, 0.65, 0.60, 0.55, 0.50, 0.45

MASS FLOW RATIO W_2/W_1

EJECTOR AREA RATIO — A_3/A_1
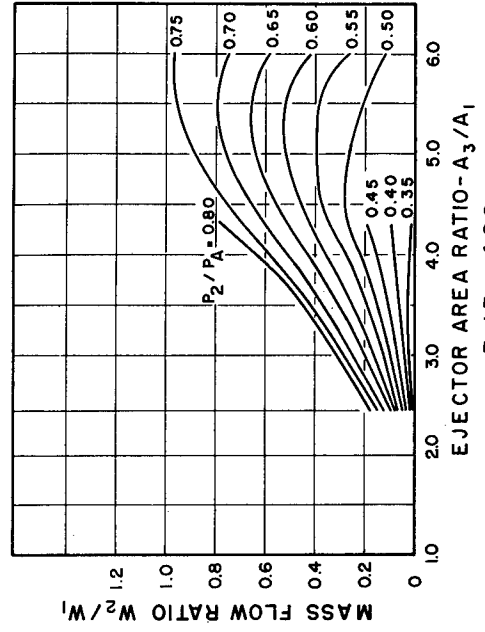
$P_1/P_A = 2.00$

EJECTOR PERFORMANCE

(WITH DIFFUSER)

FIGURE - 31

$(A_3/A_1 = 2.48)$

FIGURE - 32

$(A_3/A_1 = 4.30)$

FIGURE - 30

$(A_3/A_1 = 1.72)$

SYMBOLS- P_1/P_A		$L = 7.5 D_3$
◇ = 4.00		$\ell = 0$
◁ = 3.00		
◰ = 2.50		
◿ = 2.00		
◇ = 1.50		
◁ = 1.25		
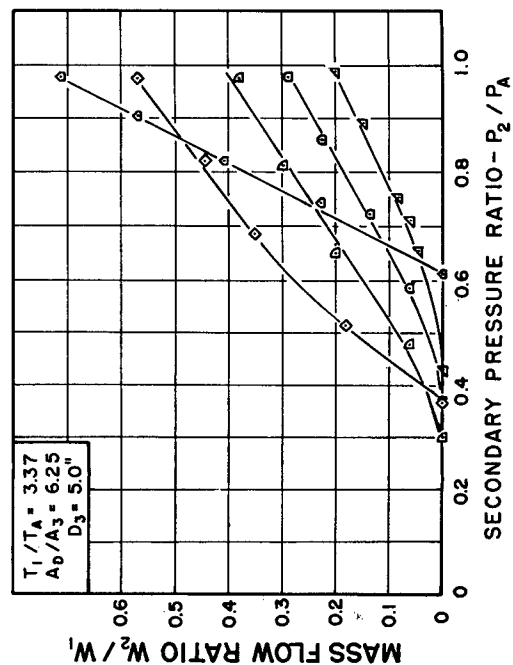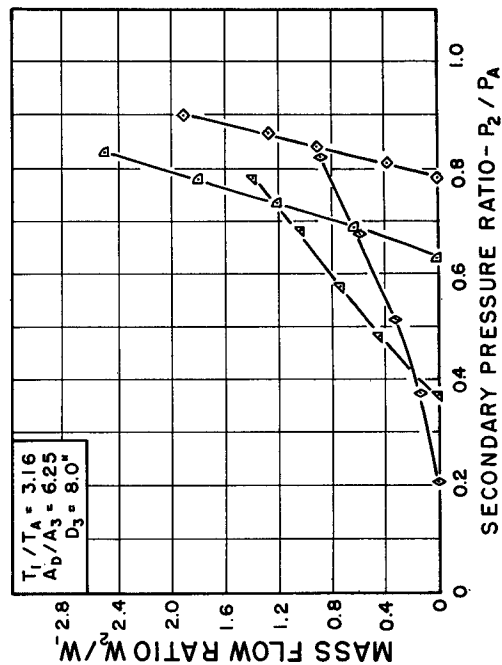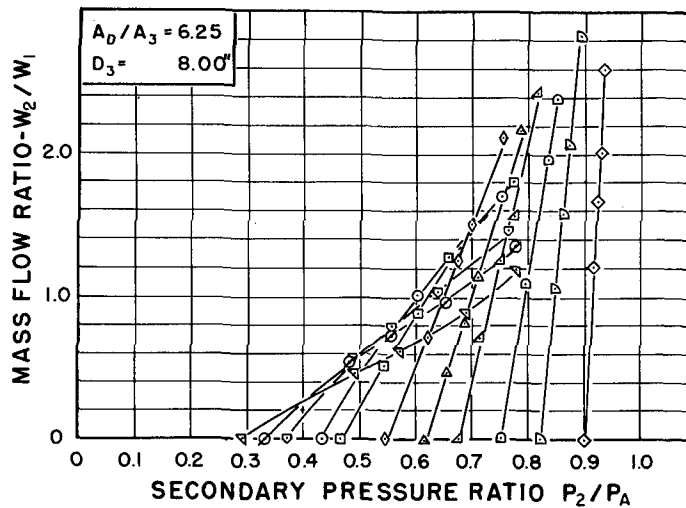
$A_3/A_1 = 8.60$
FIGURE- 33

EJECTOR PERFORMANCE
(WITH DIFFUSER)

SYMBOLS P_1/P_A	$T_1/T_A = 3.32$
▽ $P_1/P_A = 6.50$	$D_1 = 2.73"$
∅ $P_1/P_A = 6.00$	$L = 7.5 D_3$
▽ $P_1/P_A = 5.50$	$\mathfrak{L} = 0$
○ $P_1/P_A = 5.00$	
□ $P_1/P_A = 4.50$	
◇ $P_1/P_A = 4.00$	
△ $P_1/P_A = 3.50$	
◁ $P_1/P_A = 3.00$	
⌂ $P_1/P_A = 2.50$	
▷ $P_1/P_A = 2.00$	
◇ $P_1/P_A = 1.50$	
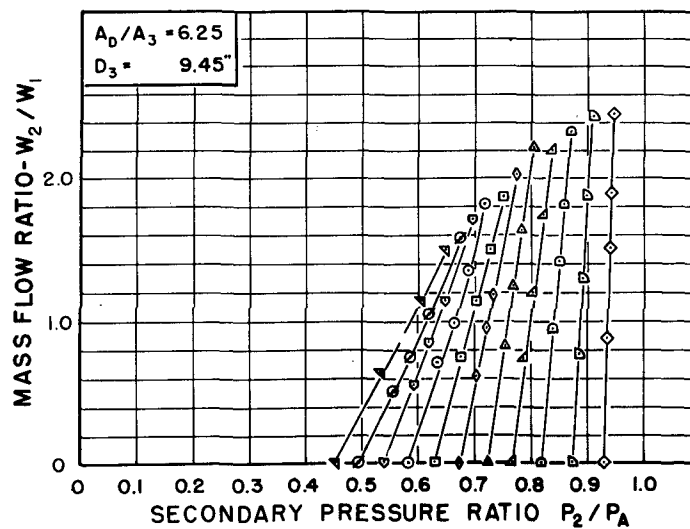
$A_3/A_1 = 12.00$

FIGURE-34
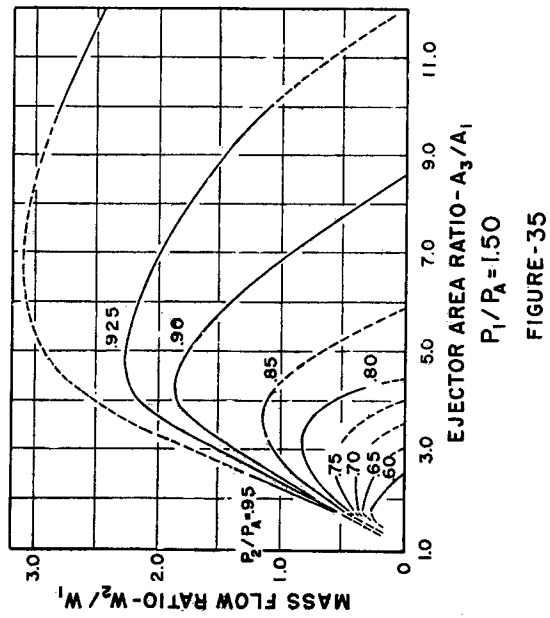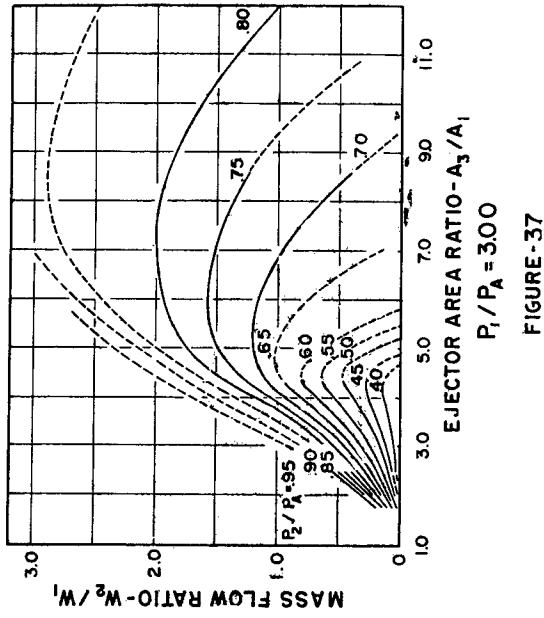
OPTIMUM EJECTOR AREA RATIO
(WITH DIFFUSER)
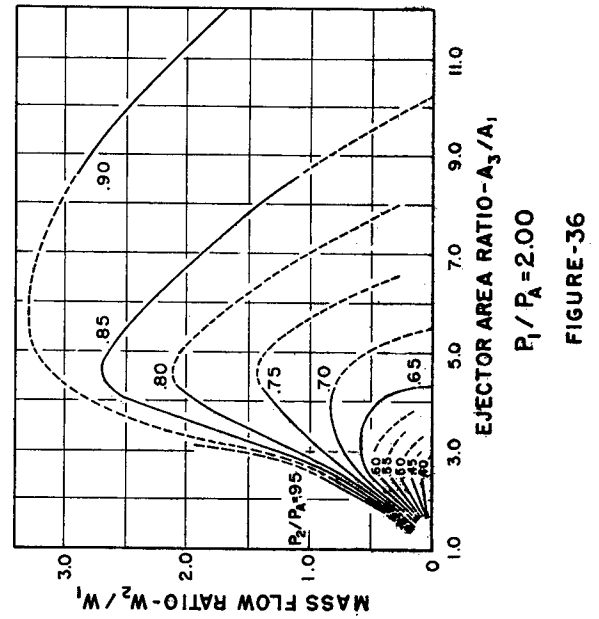
FIGURE-37 — $P_1/P_A = 3.00$
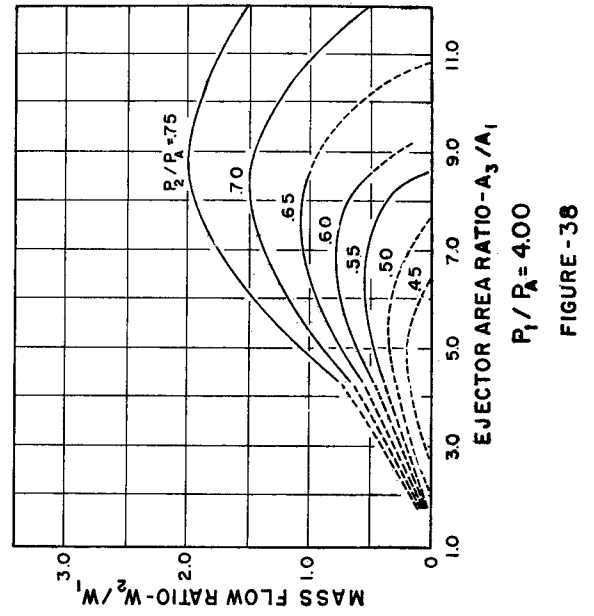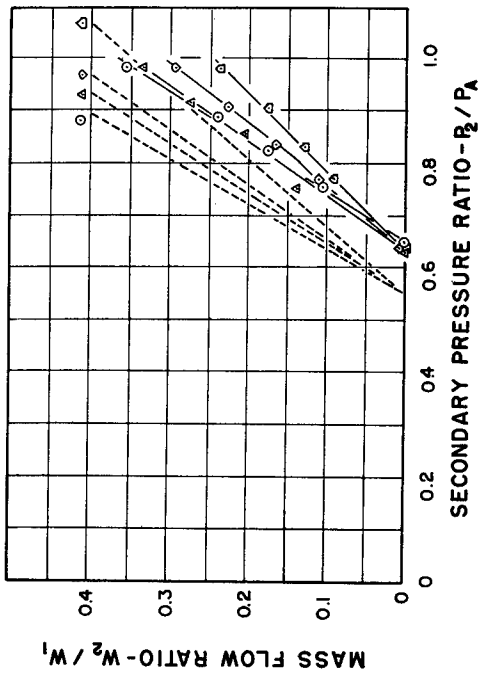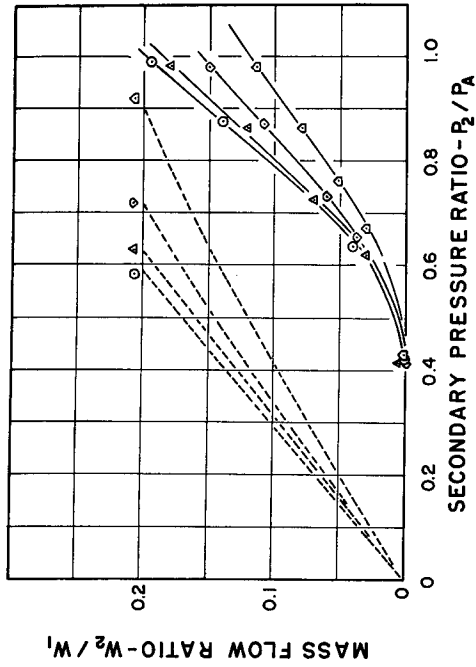
FIGURE-38 — $P_1/P_A = 4.00$

FIGURE-35 — $P_1/P_A = 1.50$

FIGURE-36 — $P_1/P_A = 2.00$

A_4/A
1.72
2.48
4.30
8.60
12.00

$T_1/T_A = 3.32$
$L = 7.5 D_3$
$\phi = 0$

THE EFFECT OF PRIMARY TEMPERATURE VARIATION ON EJECTOR PERFORMANCE
(WITHOUT DIFFUSER)

FIGURE - 41

MASS FLOW RATIO - W_2/W_1

SECONDARY PRESSURE RATIO - P_2/P_A

FIGURE - 39

MASS FLOW RATIO - W_2/W_1

SECONDARY PRESSURE RATIO - P_2/P_A

FIGURE - 42

GROSS THRUST - F_e - LBS

SECONDARY PRESSURE RATIO - P_2/P_A

SYMBOLS - T_1/T_A

O = 3.19   ◇ = 1.65   △ = 1.00
△ = 2.42   ◁ = 1.00
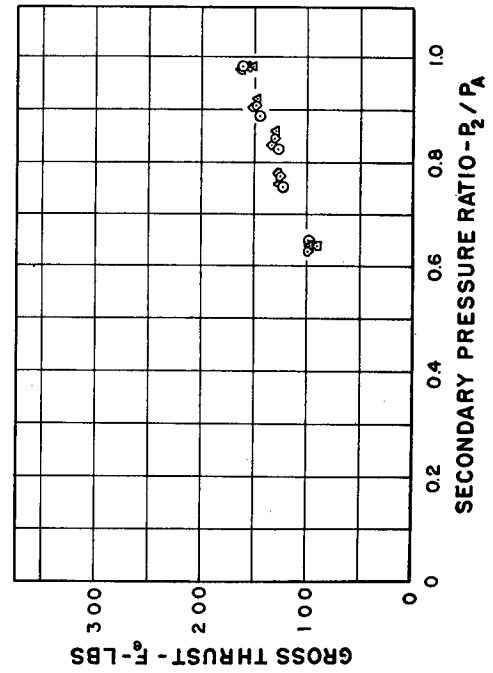
P_1/P_A = 3.00

$D_3 = 5"$
$A_3/A_1 = 1.72$
$L = 7.5 D_3$
$\ell = 0$

--- THEORETICAL

FIGURE - 40
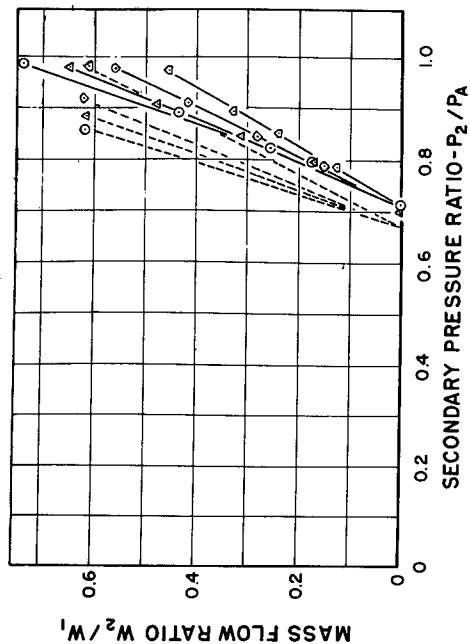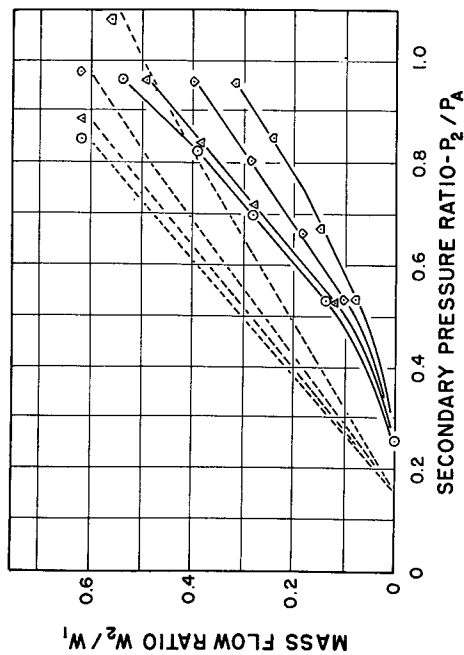
GROSS THRUST - F_e - LBS

SECONDARY PRESSURE RATIO - P_2/P_A

SYMBOLS - T_1/T_A

O = 3.26   ◇ = 1.65
△ = 2.47   ◁ = 1.00

P_1/P_A = 1.50

THE EFFECT OF PRIMARY TEMPERATURE VARIATION ON EJECTOR PERFORMANCE
(WITHOUT DIFFUSER)

$P_1/P_A = 3.0$

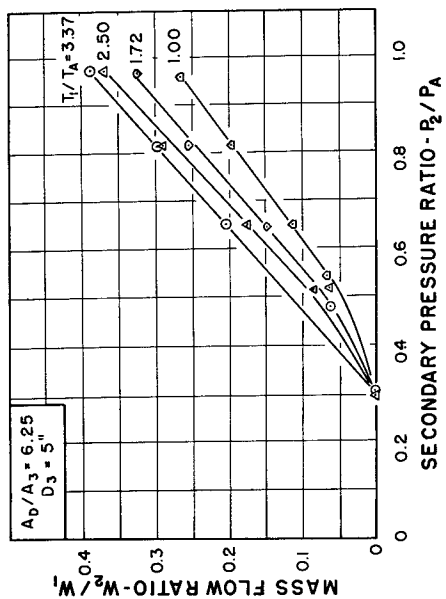**FIGURE-45**

MASS FLOW RATIO W_2/W_1

SECONDARY PRESSURE RATIO $-P_2/P_A$

$P_1/P_A = 3.0$

FIGURE-46

GROSS THRUST $-F_g$ -LBS

SECONDARY PRESSURE RATIO $-P_2/P_A$

$A_3/A_1 = 2.48$
$D_3 = 6''$
$L = 7.5 D_3$
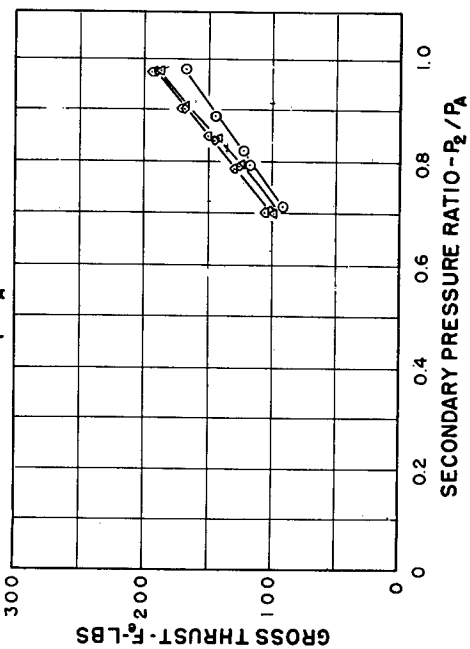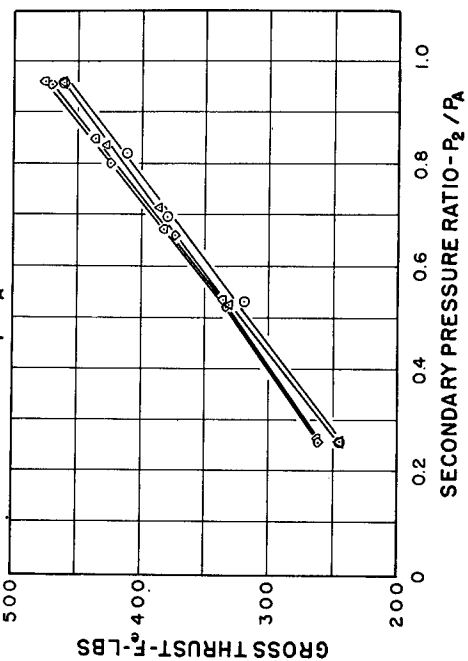
SYMBOLS $-T_1/T_A$	
O =	3.32
△ =	2.52
◇ =	1.72
◁ =	1.00

---THEORETICAL
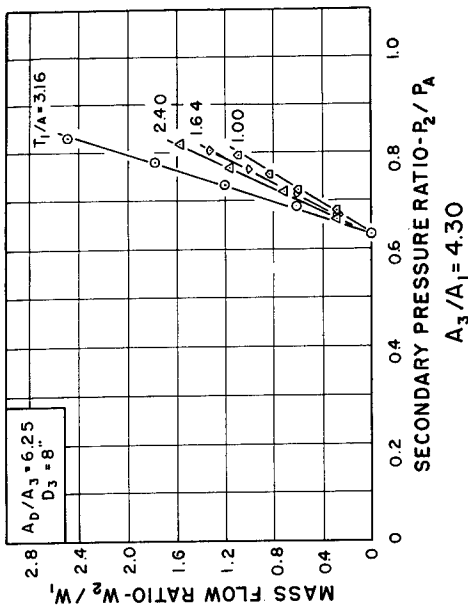
$P_1/P_A = 1.5$

FIGURE-43

MASS FLOW RATIO W_2/W_1

SECONDARY PRESSURE RATIO $-P_2/P_A$

$P_1/P_A = 1.5$

FIGURE-44

GROSS THRUST $-F_g$ -LBS

SECONDARY PRESSURE RATIO $-P_2/P_A$

THE EFFECT OF PRIMARY
TEMPERATURE VARIATION ON EJECTOR PERFORMANCE
(WITH DIFFUSER)

$P_1/P_A = 2.00$
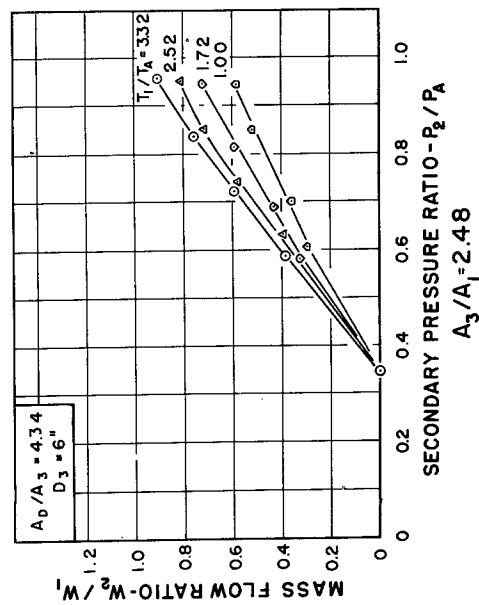$\alpha = 0$
$L = 7.5 D_3$

FIGURE - 47
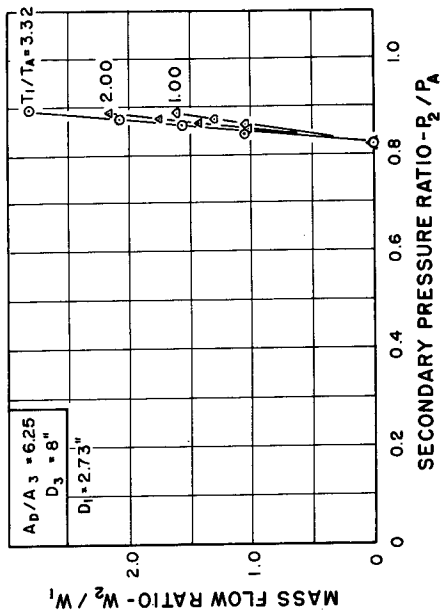
FIGURE - 48
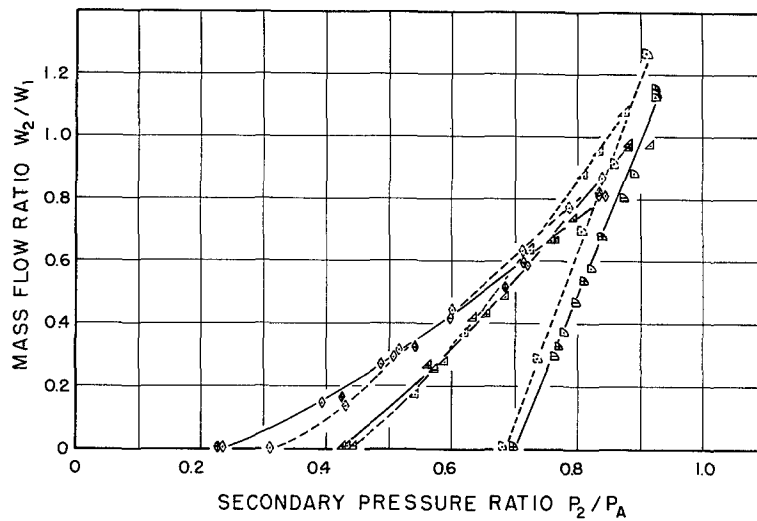
FIGURE - 49

FIGURE - 50,

FIGURE- 51

EJECTOR PERFORMANCE WITH SUPERSONIC PRIMARY NOZZLE
(WITHOUT DIFFUSER)

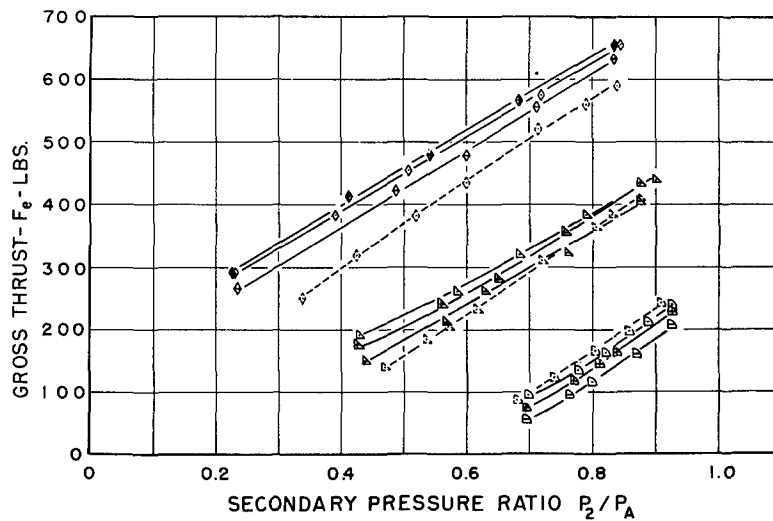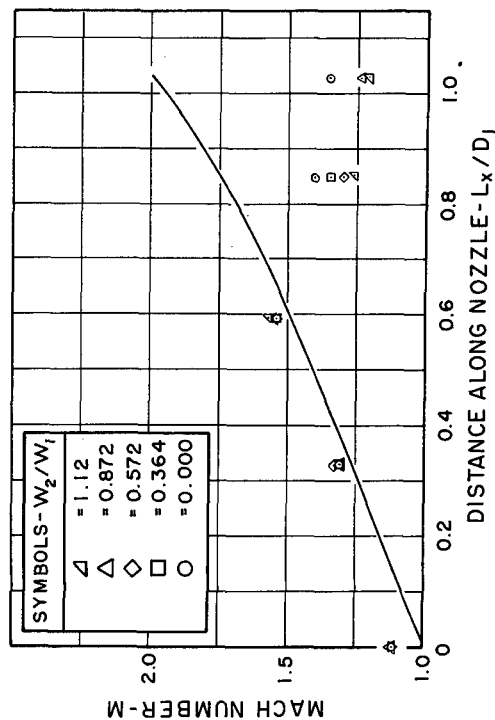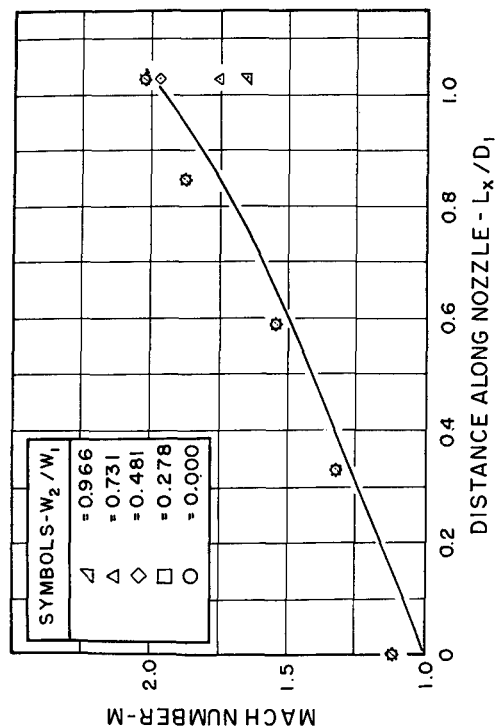| SYMBOLS		$T_1/T_A = 3.32$
$\square$ $\ell = 0$		
$\ominus$ $\ell = -.0725D_3$ } $P_1/P_A = 2.0$		$\dfrac{A_3}{A_1^*} = 4.30$
$\ominus$ $\ell = -.25D_3$		
$\triangle$ $\ell = 0$		
$\triangle$ $\ell = -.0725D_3$ } $P_1/P_A = 3.0$		$D_1^* = 3.938"$
$\triangle$ $\ell = -.25D_3$		
$\diamond$ $\ell = 0$		
$\diamond$ $\ell = -.0725D_3$ } $P_1/P_A = 4.0$		$D_3 = 8.0"$
$\oplus$ $\ell = -.25D_3$		$L = 7.5D_3$
SUPERSONIC NOZZLE EXIT MACH NO. = 2.00		
------ = SONIC NOZZLE CURVES		

FIGURE- 52
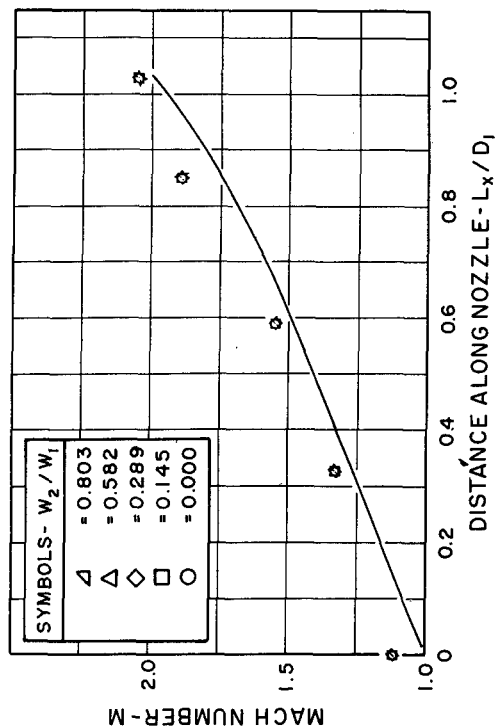
MACH NUMBER IN SUPERSONIC NOZZLE AT VARIOUS MASS FLOW RATIOS

$A_3/A_1^* = 4.30$	$D_1^* = 3.938"$
$T_1/T_A = 3.32$	$L = 7.5 D_3$
$D_3 = 8.0"$	$\ell = 0$
—— THEORETICAL CURVE	
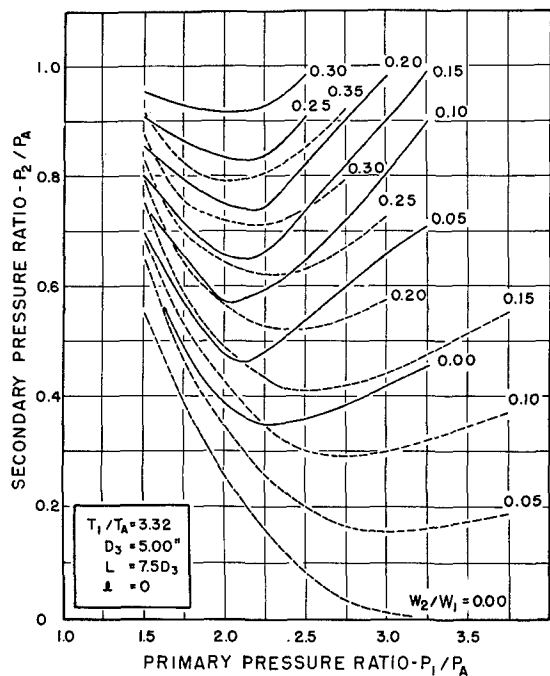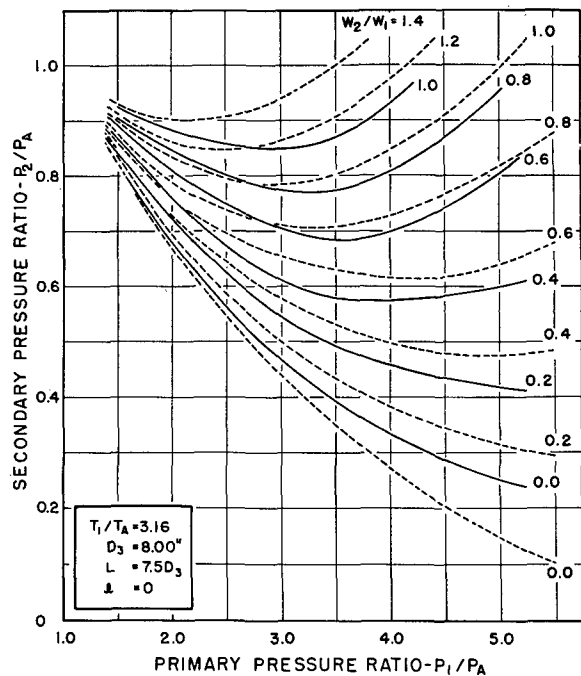
SYMBOLS - W_2/W_1	
◁	=0.966
△	=0.731
◇	=0.481
□	=0.278
○	=0.000

$P_1/P_A = 3.0$

FIGURE-54

SYMBOLS - W_2/W_1	
◁	=0.803
△	=0.582
◇	=0.289
□	=0.145
○	=0.000

$P_1/P_A = 4.0$

FIGURE-55

SYMBOLS - W_2/W_1	
◁	=1.12
△	=0.872
◇	=0.572
□	=0.364
○	=0.000

$P_1/P_A = 2.0$

FIGURE-53

FIGURE-56

$A_3/A_1 = 1.72$

$T_1/T_A = 3.32$
$D_3 = 5.00''$
$L = 7.5 D_3$
$\perp = 0$

$W_2/W_1 = 0.00$

FIGURE-58

$A_3/A_1 = 4.30$

$T_1/T_A = 3.16$
$D_3 = 8.00''$
$L = 7.5 D_3$
$\perp = 0$

EJECTOR PUMPING PERFORMANCE

—— EXPERIMENTAL CURVES

----- THEORETICAL CURVES

FIGURE-57

$A_3/A_1 = 2.48$

$T_1/T_A = 3.32$
$D_3 = 6.00''$
$L = 7.5 D_3$
$\perp = 0$

$W_2/W_1 = 0.0$

FIGURE-59

$A_3/A_1 = 6.00$

$T_1/T_A = 3.32$
$D_3 = 9.45''$
$L = 7.5 D_3$
$\perp = 0$

EJECTOR THRUST PERFORMANCE

— EXPERIMENTAL CURVES

--- THEORETICAL CURVES

$T_1/T_a = 3.16$
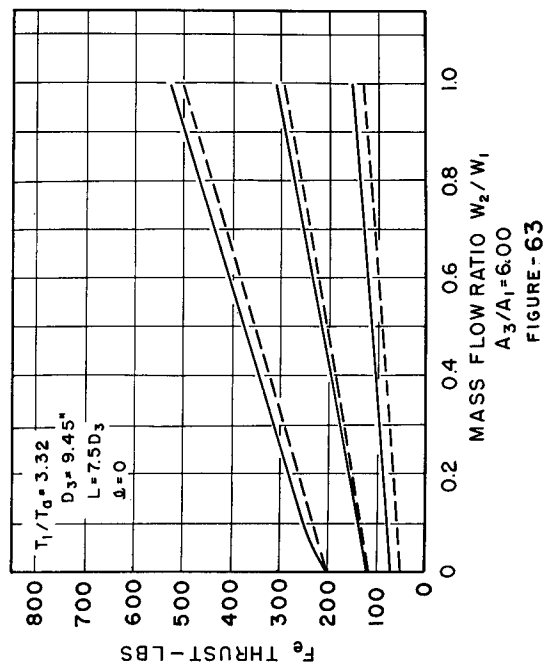$D_3 = 8.00"$
$L = 7.5 D_3$
$\lambda = 0$

MASS FLOW RATIO W_2/W_1
$A_3/A_1 = 4.30$

F_e THRUST-LBS

FIGURE-62

$T_1/T_a = 3.32$
$D_3 = 9.45"$
$L = 7.5 D_3$
$\lambda = 0$

MASS FLOW RATIO W_2/W_1
$A_3/A_1 = 6.00$

F_e THRUST-LBS

FIGURE-63

$T_1/T_a = 3.32$
$D_3 = 5.00"$
$L = 7.5 D_3$
$\lambda = 0$

MASS FLOW RATIO W_2/W_1
$A_3/A_1 = 1.72$

F_e THRUST-LBS

FIGURE-60

$T_1/T_a = 3.32$
$D_3 = 6.00"$
$L = 7.5 D_3$
$\lambda = 0$

MASS FLOW RATIO W_2/W_1
$A_3/A_1 = 2.48$

F_e THRUST-LBS
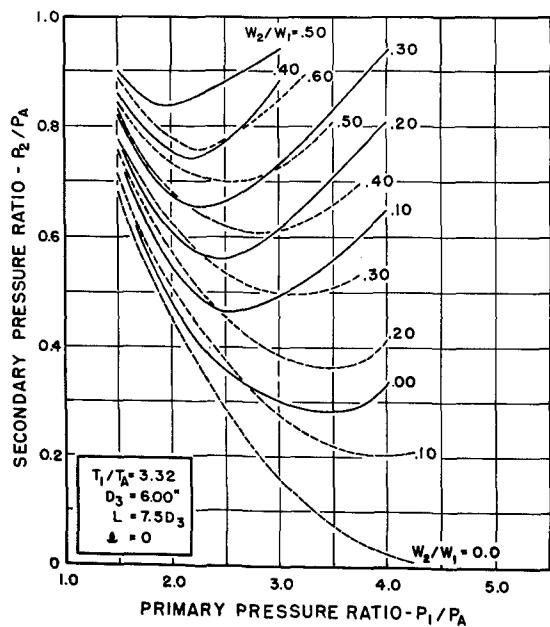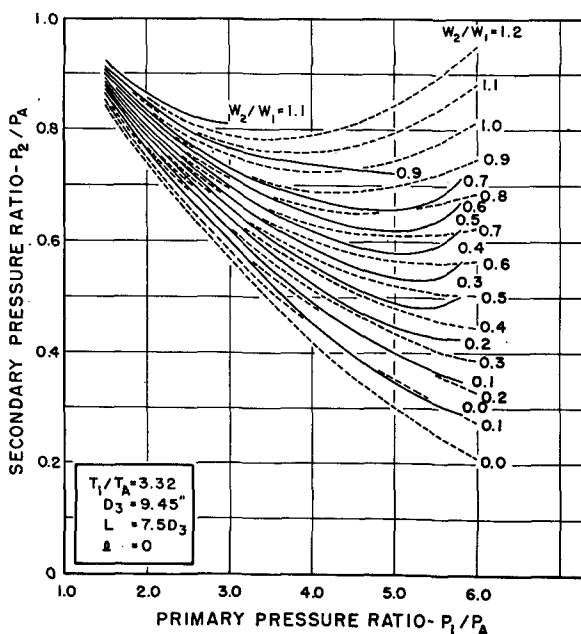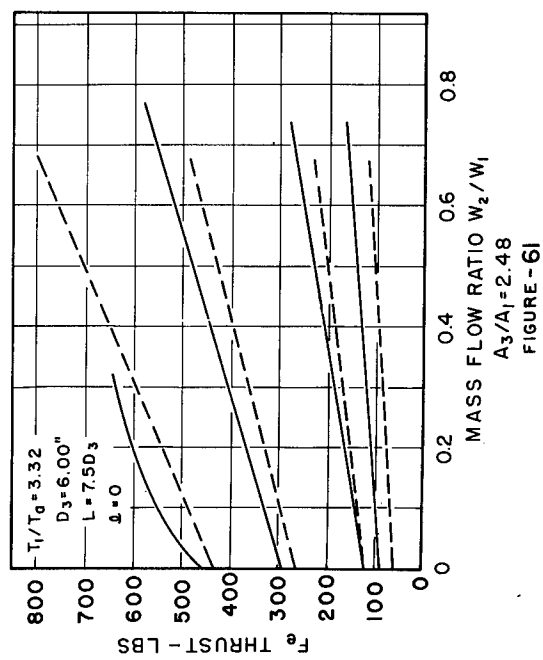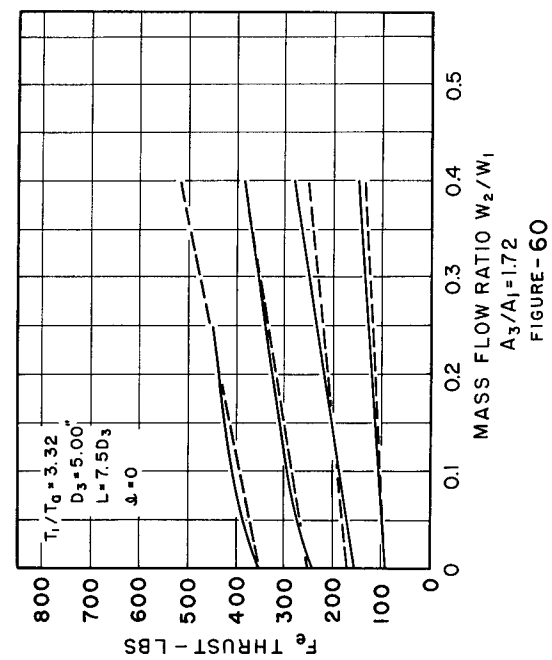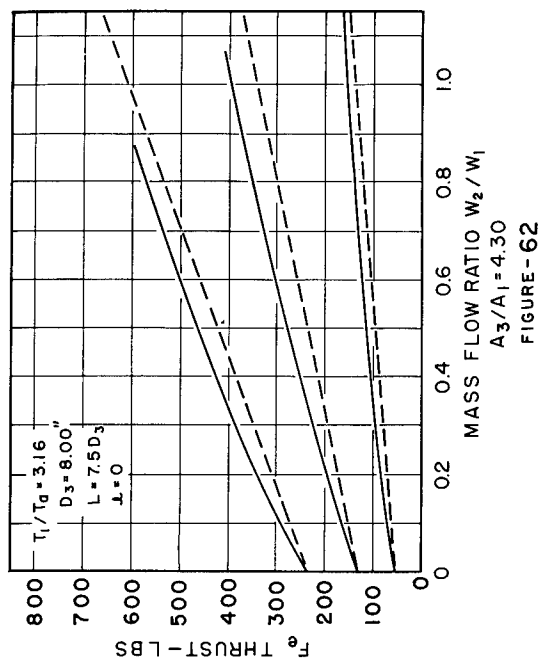
FIGURE-61

EXIT TOTAL PRESSURE RATIO ACROSS MIXING TUBE

A₃/A₁ = 4.30
D₃ = 8.00"
L = 7.5 D₃
ℓ = 0

$A_3/A_1 = 4.30$
$D_3 = 8.00''$
$L = 7.5\,D_3$
$\ell = 0$

SYMB.	W_2/W_1	P_2/P_A
△	1.060	0.872
□	0.490	0.706
◇	0.000	0.513

$T_1/T_2 = 3.16$
--·-- THEORETICAL

DISTANCE ACROSS MIXING TUBE D_x/D_3

EXIT TOTAL PRESSURE RATIO P_A/P_3

$P_1/P_A = 2.75$

FIGURE- 65

SYMB.	W_2/W_1	P_2/P_A
△	1.320	0.931
□	0.691	0.844
◇	0.000	0.742

$T_1/T_2 = 3.29$
--·-- THEORETICAL

DISTANCE ACROSS MIXING TUBE D_x/D_3

EXIT TOTAL PRESSURE RATIO P_A/P_3

$P_1/P_A = 1.75$

FIGURE- 64

SYMB.	W_2/W_1	P_2/P_A
△	0.876	0.842
□	0.454	0.624
◇	0.000	0.359

$T_1/T_2 = 3.16$
--·-- THEORETICAL

DISTANCE ACROSS MIXING TUBE D_x/D_3

EXIT TOTAL PRESSURE RATIO P_A/P_3

$P_1/P_A = 3.75$

FIGURE- 66

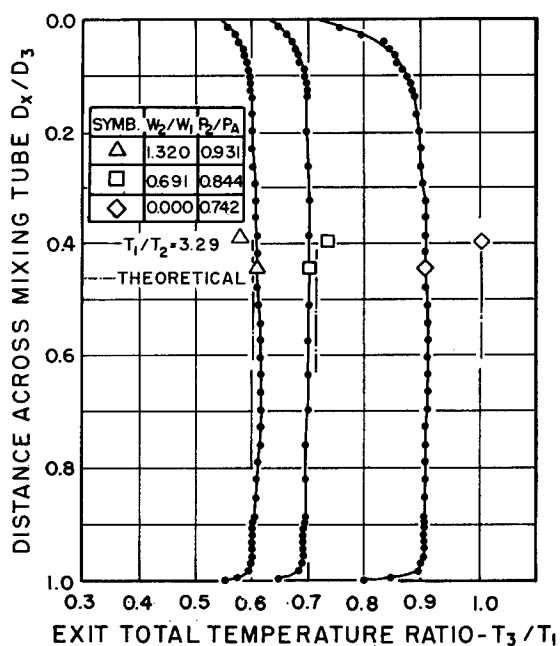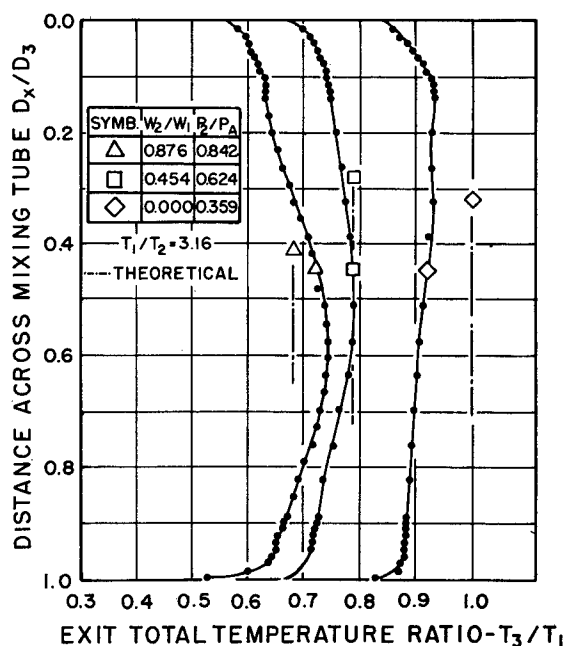# EXIT TOTAL TEMPERATURE RATIO ACROSS MIXING TUBE

A₃/A₁=4.30
D₃=8.00"
L =7.5D₃
ʟ =0
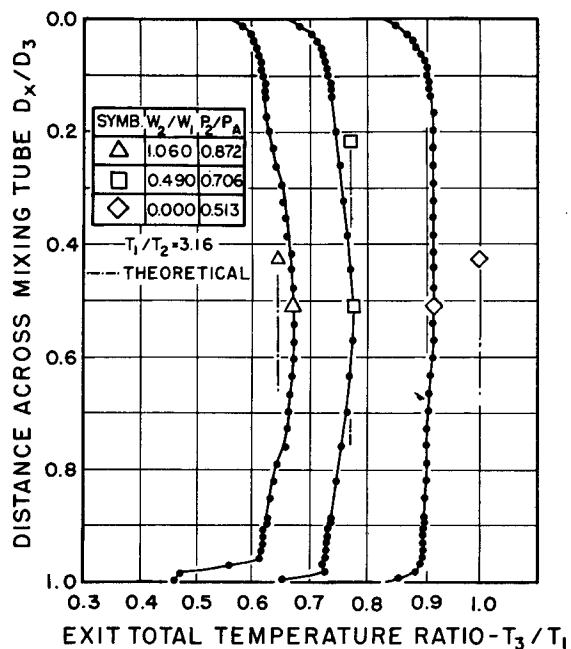
$P_1/P_A = 2.75$

FIGURE-68

$P_1/P_A = 1.75$

FIGURE-67

$P_1/P_A = 3.75$
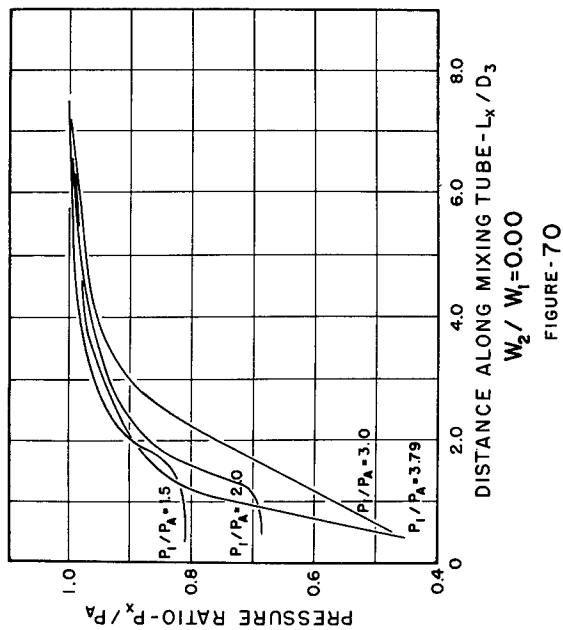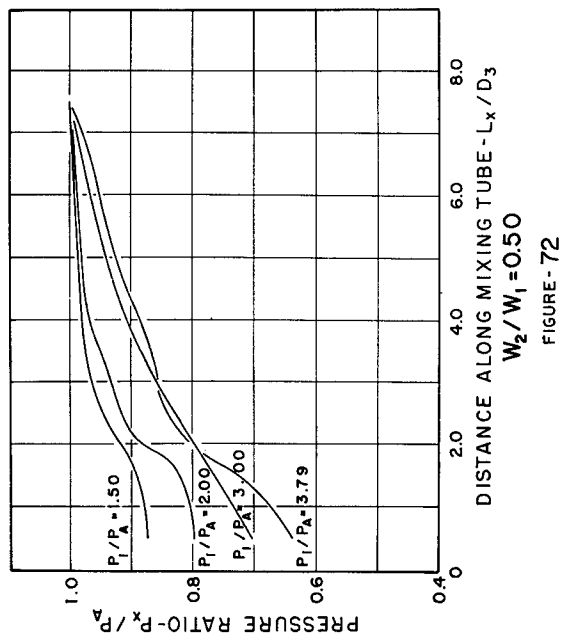
FIGURE-69

EFFECT OF PRIMARY PRESSURE VARIATION
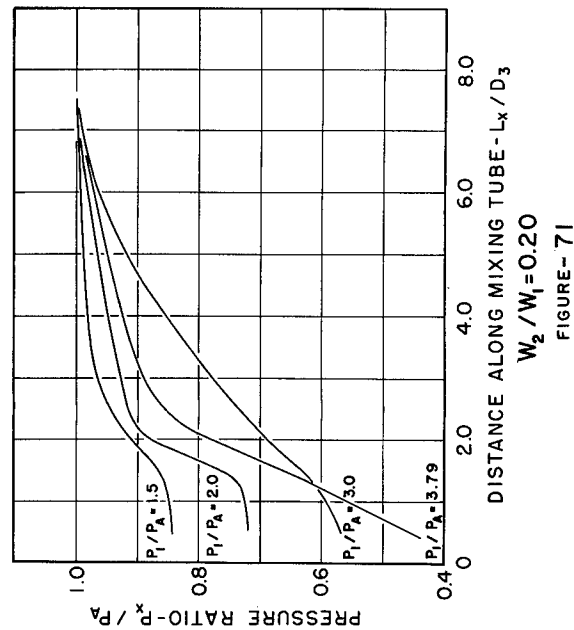# ON THE STATIC PRESSURE DISTRIBUTION

FIGURE-70

$W_2/W_1 = 0.00$

$P_1/P_A = 1.5$
$P_1/P_A = 2.0$
$P_1/P_A = 3.0$
$P_1/P_A = 3.79$

DISTANCE ALONG MIXING TUBE - L_x/D_3

PRESSURE RATIO - P_x/P_A

FIGURE-72

$W_2/W_1 = 0.50$

$P_1/P_A = 1.50$
$P_1/P_A = 2.00$
$P_1/P_A = 3.00$
$P_1/P_A = 3.79$

DISTANCE ALONG MIXING TUBE - L_x/D_3

PRESSURE RATIO - P_x/P_A

FIGURE-71

$W_2/W_1 = 0.20$

$P_1/P_A = 1.5$
$P_1/P_A = 2.0$
$P_1/P_A = 3.0$
$P_1/P_A = 3.79$

DISTANCE ALONG MIXING TUBE - L_x/D_3

PRESSURE RATIO - P_x/P_A

FIGURE-73

$W_2/W_1 = 0.80$

$P_1/P_A = 1.50$
$P_1/P_A = 2.00$
$P_1/P_A = 3.00$
$P_1/P_A = 3.79$

DISTANCE ALONG MIXING TUBE - L_x/D_3

PRESSURE RATIO - P_x/P_A

$A_3/A_1 = 4.30$
$T_1/T_A = 3.07$
$D_3 = 8''$
$L = 7.5D_3$
$\ell = 0$